GPU Nuclear

GPU Nuclear Corporation
Post Office Box 480
Route 441 South
Middletown, Pennsylvania 17057-0191
717 944-7621
TELEX 84-2386
Writer's Direct Dial Number:

(717) 948-8461

4410-87-L-0052
Document ID D133P

May 7, 1987

US Nuclear Regulatory Commission
Attn: Document Control Desk
Washington, DC 20555

Dear Sirs:

Three Mile Island Nuclear Station, Unit 2 (TMI-2)
Operating License No. DPR-73
Docket No. 50-320
Annual Update of the Defueling Canister Technical Evaluation Report

Pursuant to NRC Letter dated February 4, 1982, attached for your information is the annual update to the Technical Evaluation Report for the TMI-2 Defueling Canisters. This update incorporates the use of "deep-bed" filters, the use of coagulants and diatomaceous earth, and the capability to draw deep-suction with the Defueling Water Cleanup System. These issues have been addressed previously in the following correspondence:

- NRC Letter NRC/TMI-87-027 dated March 27, 1987
- GPU Nuclear letter 4410-87-L-0024 dated February 20, 1987
- GPU Nuclear letter 4410-87-L-0021 dated February 20, 1987
- NRC Letter NRC/TMI-87-02 dated January 15, 1987
- GPU Nuclear letter 4410-86-L-0216 dated December 31, 1986
- NRC Letter NRC/TMI-86-119 dated December 22, 1986
- GPU Nuclear letter 4410-86-L-0213 dated December 15, 1986
- GPU Nulcear letter 4410-86-L-0173 dated September 26, 1986
- NRC Letter NRC/TMI-86-066 dated July 9, 1986
- GPU Nuclear letter 4410-86-L-0104 dated June 30, 1986

8705120366 870507
PDR ADOCK 05000320
P PDR

A001
1/1

Additionally, this update revises the quantity of recombiner catalyst required to be exposed in dewatered canisters and the minimum time required for a canister dewatered to 25% void volume to achieve its design pressure.

Sincerely,

F. R. Standerfer
Director, TMI-2

FRS/RDW/eml

Attachment

cc: Regional Administrator - Region 1, Mr. W. T. Russell
Director - TMI-2 Cleanup Project Directorate, Dr. W. D. Travers

GPU Nuclear

TER 3527-016 REV 3

ISSUE DATE May 1987

☐ ITS
☒ NSR
☐ NITS

DIVISION

TECHNICAL EVALUATION REPORT

FOR

Defueling Canisters

ORIGINATOR Richard E Sheppard DATE 4/14/87

COG ENG [illegible] DATE 4/17/87

RTR [illegible] DATE 4/22/87

COG ENG MGR. [illegible] DATE 4/24/87

8705120374 870507
PDR ADOCK 05000320
P PDR

Rev.	SUMMARY OF CHANGE	Approval	Date
0	Issued for initial use.		3/85
1	Update to incorporate design change from vibrapacked B_4C powder to sintered B_4C pellets, discussion if maximum particle size expected in filter canister, increase in load limit on fuel canister lower support plate from 350 to 550 lbs., addition of k_{eff} criteria for plant accident condition (0.99), discussion of effects on criticality analyses caused by a) change to B_4C pellets, b) lower storage pool water temperature, and c) fuel particle size, addition of section regarding hydrogen controls within the canister.		9/85
2	Update to incorporate change to allow fuel particles greater than standard whole pellets size to introduced into knockout and fuel canisters. Specific reference to the Fines/Debris Vacuum System was also deleted from Section 2.3 to allow additional application of the knockout canister.		3/86
3	Update to incorporate use of "deep-bed" filters, coagulants and diatomaceous earth in DWCS, to correct statements regarding the exposed quantity of catalyst in dewatered canisters, to present canister pressure after 25% void volume dewatering, and to refelct the use of deep suction in the DWCS.		5/87

TABLE OF CONTENTS

SECTION		PAGE
1.0	INTRODUCTION	4
1.1	Purpose	4
1.2	Scope	4
2.0	CANISTER DESCRIPTION	4
2.1	Codes and Standards	5
2.2	Fuel Canister	6
2.3	Knockout Canister	7
2.4	Filter Canister	8
3.0	TECHNICAL EVALUATION	16
3.1	Canister Structural Evaluation	16
3.2	Canister Criticality Evaluation	18
3.3	Canister Hydrogen Control Evaluation	21
4.0	RADIOLOGICAL CONSIDERATIONS	27
5.0	10CFR 50.59 EVALUATION	27
6.0	CONCLUSION	28
7.0	REFERENCES	28

ATTACHMENTS

1. TMI-2 Transfer System Criticality Technical Report

2. Assessment of a Drained Pool Scenario

1.0 INTRODUCTION

Canisters are required during the defueling at TMI-2 to retain core debris ranging from very small fines to partial length fuel assemblies. These canisters provide effective long term storage of the TMI-2 core debris. Three types of canisters are required to support the defueling system to be used at TMI-2: filter, knockout, and fuel canisters.

1.1 Purpose

The purpose of this report is to show that the canisters are designed to remain safe under normal operation and handling conditions as well as postulated drop accidents and storage. Section 2.0 of this report describes the three types of canisters. Section 3.0 addresses the safety of the canister design considering design drop analyses and drop tests and criticality analyses. Requirements for spacing of the canisters in an array under normal conditions are also addressed. Section 4.0 outlines the radiological concerns associated with the handling and storage of the canisters. Section 5.0 draws conclusions about the safe operation and handling of the canisters.

1.2 Scope

This report addresses only those safety issues associated with the loading, handling and storage of the canisters as related to canister design. Analyses of the design drop considers only the effect of that drop on a canister; damage to other components is not considered. Actual handling of the canisters is not addressed in this report and neither are the shielding requirements for canister handling with the exception that the criticality concern associated with the use of lead shields around the canisters is addressed in Attachment 1. Also, the criticality concern associated with a drained spent fuel pool is addressed in Attachment 2. Canister performance during defueling is addressed here only as it impacts the safe use of the canister. Canister interfaces with the defueling equipment, canister handling equipment and the fuel transfer system are not covered in this report. The issues related to canister use (e.g. shielding requirements, load drops, etc.) are evaluated in the Safety Evaluation Report for Defueling of the TMI-2 Reactor Vessel (reference 3). The transportation requirements for the canisters will be separately addressed.

2.0 CANISTER DESCRIPTION

This section presents the designs of three canisters to be used in defueling TMI-2. Compatible with the RCS and spent fuel pool environment, these canisters provide long term storage of the TMI-2 core debris. In conjunction with the defueling system, the canisters will retain and encapsulate debris ranging from micron size particles to partial length fuel assemblies.

The canisters consist of a circular pressure vessel housing one of three types of internals, depending on the function of the canister. Except for the top closures, the outer shell is the same for all three types of canister design. It serves as a pressure vessel protecting against leakage of the canister contents as well as providing structural support for the neutron absorbing materials. It is designed to withstand the pressures associated with normal operating conditions. A reversed dish end is used for the lower closure head

for all of the canisters while the upper closure head design varies according to the canister's function. The canisters are non-buoyant under all storage and operational conditions.

Each canister contains a recombiner catalyst package incorporated in the upper and lower heads. The catalyst recombines the hydrogen and oxygen gases formed by radiolytic decomposition of water in the canisters.

Each canister has two pressure relief valves which are connected to the canisters using Hansen quick disconnect couplings. The low pressure relief valve has a pressure setpoint of 25 psig. The high pressure ASME code relief valve has a 150 psig setpoint.

2.1 Codes and Standards

The defueling canisters have been classified as Nuclear Safety Related for criticality control purposes.

They are designed and designated for fabrication in accordance with the following codes and standards:

ANSI/ANS 8.1 (1983)	American National Standards Institute/ American National Standard, Nuclear Criticality Safety in Operations with Fissionable Materials Outside Reactors
ANSI/ANS 8.17 (1984)	American National Standards Institute/ American National Standard, Criticality Safety Criteria for the Handling, Storage, and Transportation of LWR Fuel Outside Reactors
ANSI N45.2 (1977)	American National Standards Institute, Quality Assurance Program Requirements for Nuclear Power Plants
ANSI N45.2.2 (1972)	American National Standards Institute, Packaging, Shipping, Receiving, Storage, and Handling of Items for Nuclear Power Plants
ANSI N45.2.11 (1974)	American National Standards Institute, Quality Assurance Requirements for the Design of Nuclear Power Plants
ANSI N45.2.13 (1976)	American National Standards Institute, Quality Assurance Requirements for Control of Procure- ment of Items and Services for Nuclear Power Plants
ANSI/ASME NQA-1 (1979) Appendix 17A-1 (including ANSI/ASME NQA-1a-1981 Addenda)	Quality Assurance Program Requirements for Nuclear Power Plants, Nonmandatory Guidance on Quality Assurance Records

ANSI/ASME NQA-1 (1979) Supplement 17S-1 (including ANSI/ASME NQA-1a-1981 Addenda)	Quality Assurance Program Requirements for Nuclear Power Plants, Supplementary Requirements for Quality Assurance Records
ASME Boiler and Pressure Vessel Code, Section VIII, Part UW (lethal) (1983)	American Society of Mechanical Engineers, Pressure Vessels
ASME Boiler and Pressure Vessel Code, Section IX (1980)	American Society of Mechanical Engineers, Welding and Brazing Qualifications
ASTM A 312 (1982)	American Society for Testing and Materials, Seamless and Welded Austenitic Stainless Steel Pipe
SNT-TC-1A (1980)	American Society for Nondestructive Testing, Recommended Practice for Nondestrutive Testing, Personnel Qualification and Certification
10 CFR 21	Reporting of Defects and Noncompliance
10 CFR 50, Appendix A	General Design Criteria for Nuclear Power Plants
10 CFR 50, Appendix B	Quality Assurance Criteria for Nuclear Power Plants and Fuel Reprocessing Plants
10 CFR 72	Licensing Requirements for the Storage of Spent Fuel in an Independent Spent Fuel Storage Installation
NUREG-0612	Control of Heavy Loads at Nuclear Power Plants

2.2 Fuel Canister

The fuel canister is a receptacle for both large and small pieces of core debris to be picked up and placed in the canister. The fuel canister consists of a cylindrical pressure vessel with a flat upper closure head. It uses the same outer shell as the other canisters. Within the shell, a full length square shroud forms the internal cavity (see Figure 2.2-1). This shroud is supported at the top by a bulkhead that mates with the upper closure head (see Figure 2.2-2). Both the shroud and core debris rest on a support plate that is welded to the shell. The support plate has impact plates attached to absorb canister drop loads and payload drop loads.

The shroud assembly consists of a pair of concentric square stainless steel plates seal welded to completely enclose four sheets of Boral, a neutron absorbing material (see Figure 2.2-1). The shroud internal dimensions are larger than the cross section of an undamaged fuel assembly. The shroud external dimensions are slightly smaller than the

inner diameter of the canister, thus providing support at the shroud corners for lateral loads. The void area outside of the shroud is filled with a cement/glass bead mixture to the maximum extent practical to eliminate migration of the debris to an area outside of the shroud during a design basis accident.

The upper closure head is attached to the canister by eight equally spaced bolts. These bolts are designed for the design pressure loads, handling loads, and postulated impact force due to shifting of the canister contents during an in-plant load drop or a shipping accident.

2.3 Knockout Canister

The knockout canister, Figure 2.3-1, will be used as part of the vacuuming systems. Flow fittings are 2" cam and groove type similar to the filter canister fittings and are capped or plugged after use. Externally, the knockout canister is similar to the other canisters, using the same outer shell design. It also incorporates the same handling tool interface.

The internals module for the knockout canister is supported from a lower header welded to the outer shell. An array of four outer neutron absorber rods around a central neutron absorber rod is located in the canister for criticality control. The four outer rods are 1.315" O.D. tubes filled with sintered B_4C pellets.

The central absorber rod is comprised of an outer strongback tube surrounding a 2.125" O.D. tube filled with sintered B_4C pellets. Lateral support for the neutron absorber rods and center assembly is provided by intermediate support plates.

The influent flow is directed tangentially along the inner diameter of the shell, setting up a swirling action of the water within the canister. The large particulates settle out and the water moves upwards, exiting the canister through a machined outlet in the head. A full flow screen ensures that particles larger than 850 microns will not escape from the knockout canister. This screen has been designed to withstand the maximum pressure differential across the screen that can be developed by the vacuum system equipment.

A number of knockout canisters have been modified for use as "deep-bed" filters. The modifications include:

- Cutting the existing inlet tube below the support ring.
- Adding a 2" outer diameter stainless steel pipe as an outlet tube.
- Sizing the support ring to accommodate the outlet tube.
- Extending the outlet tube down to about 1"above the bottom plate with the tube being routed through the gaps formed by two adjacent legs of the support spiders.
- The bottom 12" of the outlet tube has multiple 1/4" to 3/8" holes and is covered with a 100 mesh stainless steel screen.
- Diatomaceous earth (d.e.) and/or sand is added as the filter media.

These "deep-beds" were originally planned for service in the Defueling Water Cleanup System (DWCS). However, testing proved them to be not beneficial and are currently being planned for use as the canister Dewatering System filters.

2.4 Filter Canister

As part of either the DWCS or the Fines/Debris Vacuum System, the filter canisters are designed to remove small debris particles from the water. Externally, it is similar to the other canister types. The filter assembly bundle that fits inside the canister shell was designed to remove particulates down to 0.5 (nominal) microns. Flow into and out of the filter canister is through 2 1/2" cam and groove quick disconnect fittings (Figure 2.4-1).

The internal filter assembly bundle consists of a circular cluster of 17 filter elements, a drain line and a neutron absorber assembly (Figure 2.4-2). The influent enters the upper plenum region, flows down past the support plate, through the filter media and down the filter element drain tube to the lower sump. The flow is from outside to inside with the particulate remaining around the outer perimeter of the filter elements. The filtered water exits the canister via the drain line.

A filter element consists of 11 modules. Each module consists of pleated filter media forming an annulus around a central, perforated drain tube (Figure 2.4-3). Fabricated from a porous stainless steel material, the media is pre-coated with a sintered metal powder to control pore size. Bands are placed around the outer perimeter of the pleated filter media to restrict the unfolding of the pleats.

The filter assembly bundle is held in place by an upper support plate and lower header. The lower header is welded to the outer shell of the canister to provide a boundary between the primary and secondary side of the filter system. The upper header is equipped with a series of openings to allow for the passage of the influent into the filter section of the canister and to protect the filter media from direct impingement of particles carried in the influent flow. Six tie rods position the upper plate axially relative to the lower support plate.

The filter canister has a central neutron absorber rod that is comprised of an outer strong back tube surrounding a 2.125" O.D. tube filled with sintered B_4C pellets.

The filter canisters are not expected to contain significant quantities of fuel particles larger than 850 microns. The filter canisters are used with the DWCS and the defueling vacuum system. The DWCS is used to process both spent fuel pool/fuel transfer canal water and reactor coolant system (RCS) water. In the RCS, the DWCS suction is located in the upper region of the reactor vessel, where large fuel debris (i.e., >850u) would not be expected to be suspended in solution. The DWCS has been modified to allow suction from the Reactor Vessel annulus at approximately the 296' elevation. At this lower elevation, it is possible that larger than 850 micron size particles may be introduced into the filter canisters. However, a screen has been placed in the inlet pipe to the filter canister to prevent these larger particles from entering the filter canisters. The spent fuel pool/fuel transfer canal is not expected to contain significant quantities of fuel particles larger than 850 microns. Consequently, the DWCS filter canisters are not expected to contain significant quantities of fuel particles larger than 850 microns.

When the filter canisters are used in conjunction with the defueling vacuum system, they are located downstream of the knockout canisters. Proof of principle testing (Reference 11) has shown that for the planned vacuum system flowrates, minimal quantities, if any, of 850 micron or larger sized particles would be carried out of the knockout canister. Additionally, the discharge of the knockout canisters are equipped with a 841 micron screen to prevent larger fuel particles from exiting the knockout canister. Thus the vacuum system filter canisters are not expected to contain significant quantities of fuel particles larger than 850 microns.

FIGURE 2.2-1

Fuel Canister

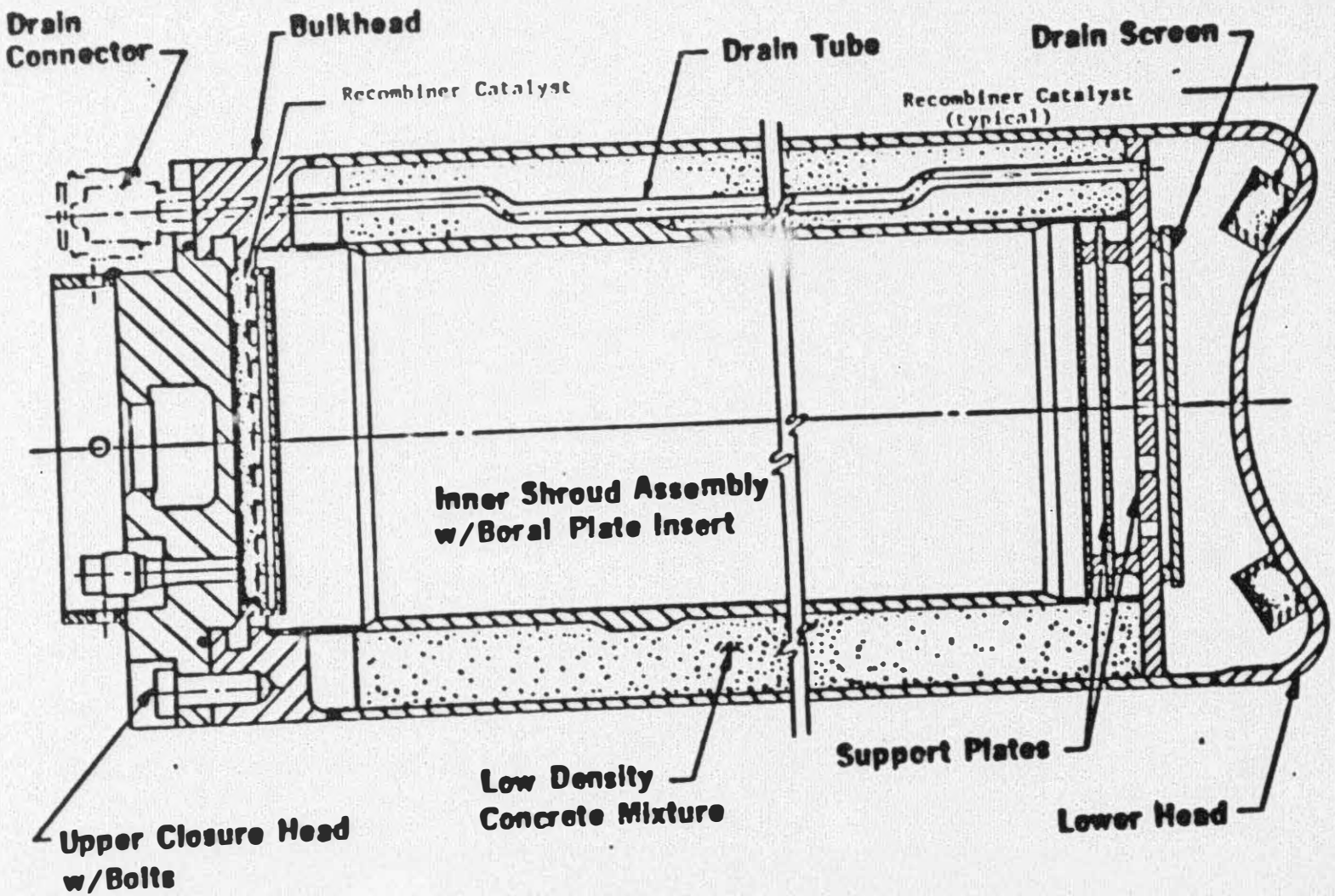

3527-016

Rev. 1

FIGURE 2.2-2

Fuel Canister Bulkhead View

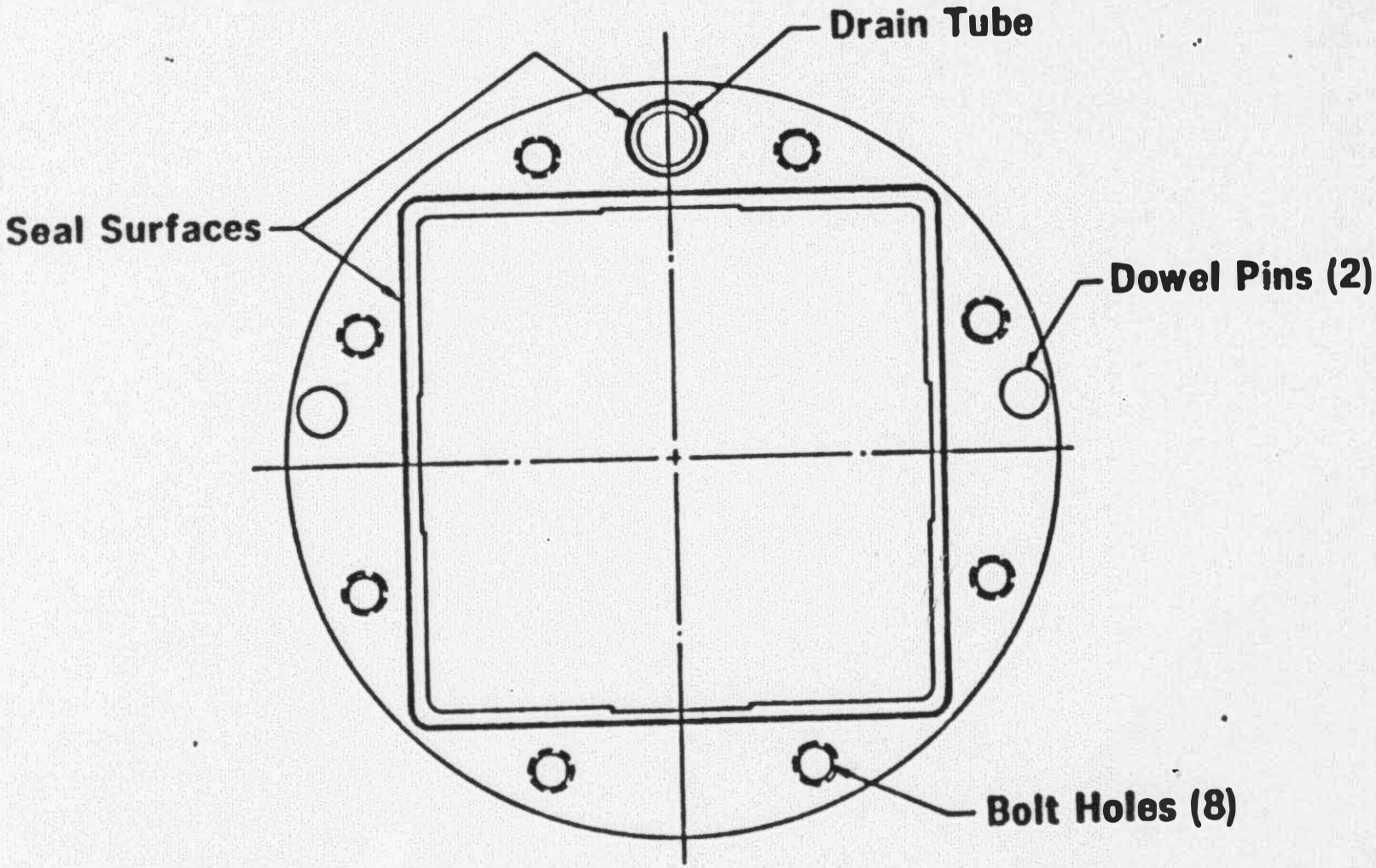

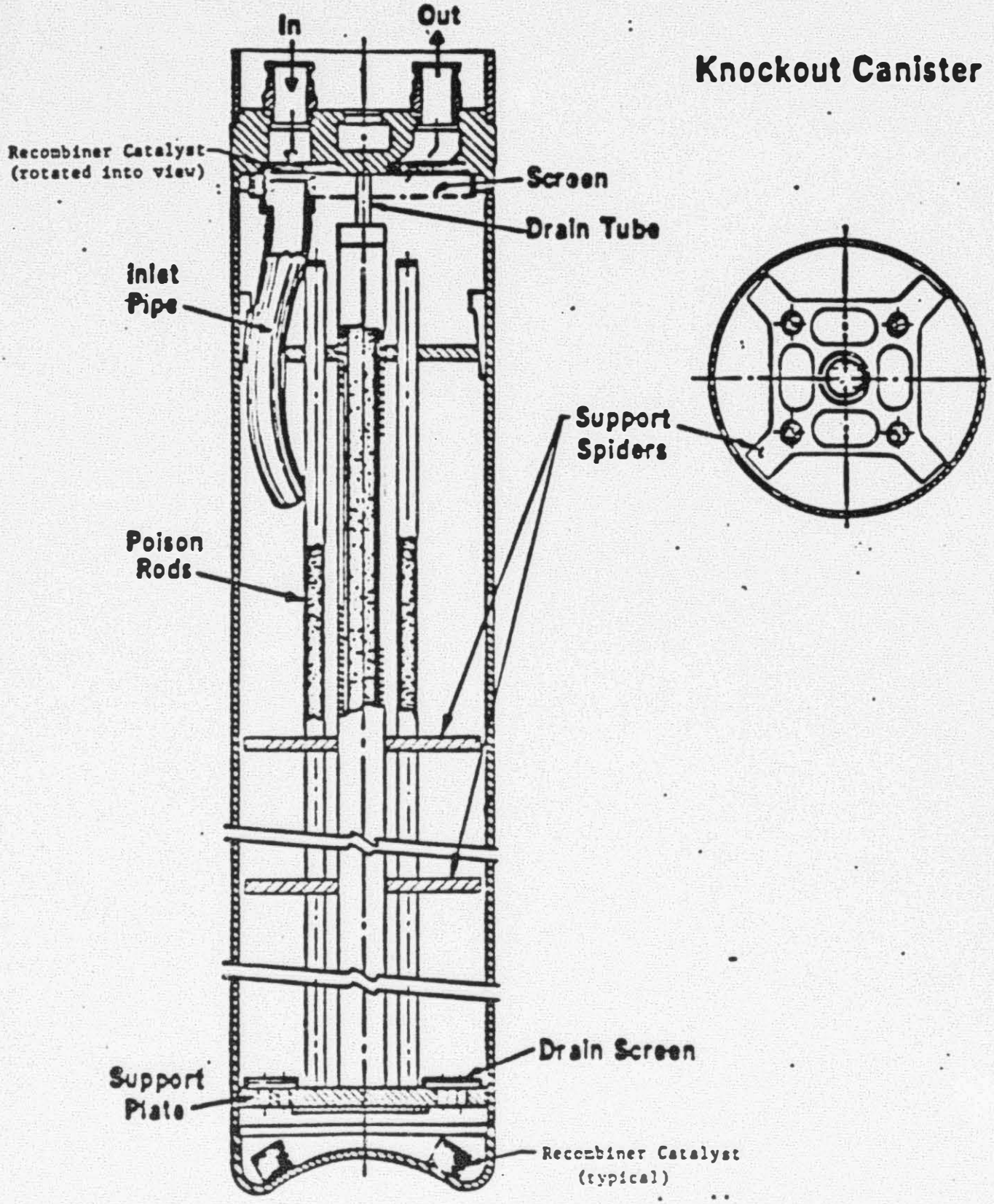
Knockout Canister
In
Out
Recombiner Catalyst
(rotated into view)
Screen
Drain Tube
Inlet
Pipe
Support
Spiders
Poison
Rods
Drain Screen
Support
Plate
Recombiner Catalyst
(typical)

FIGURE 2.4-1

Filter Canister

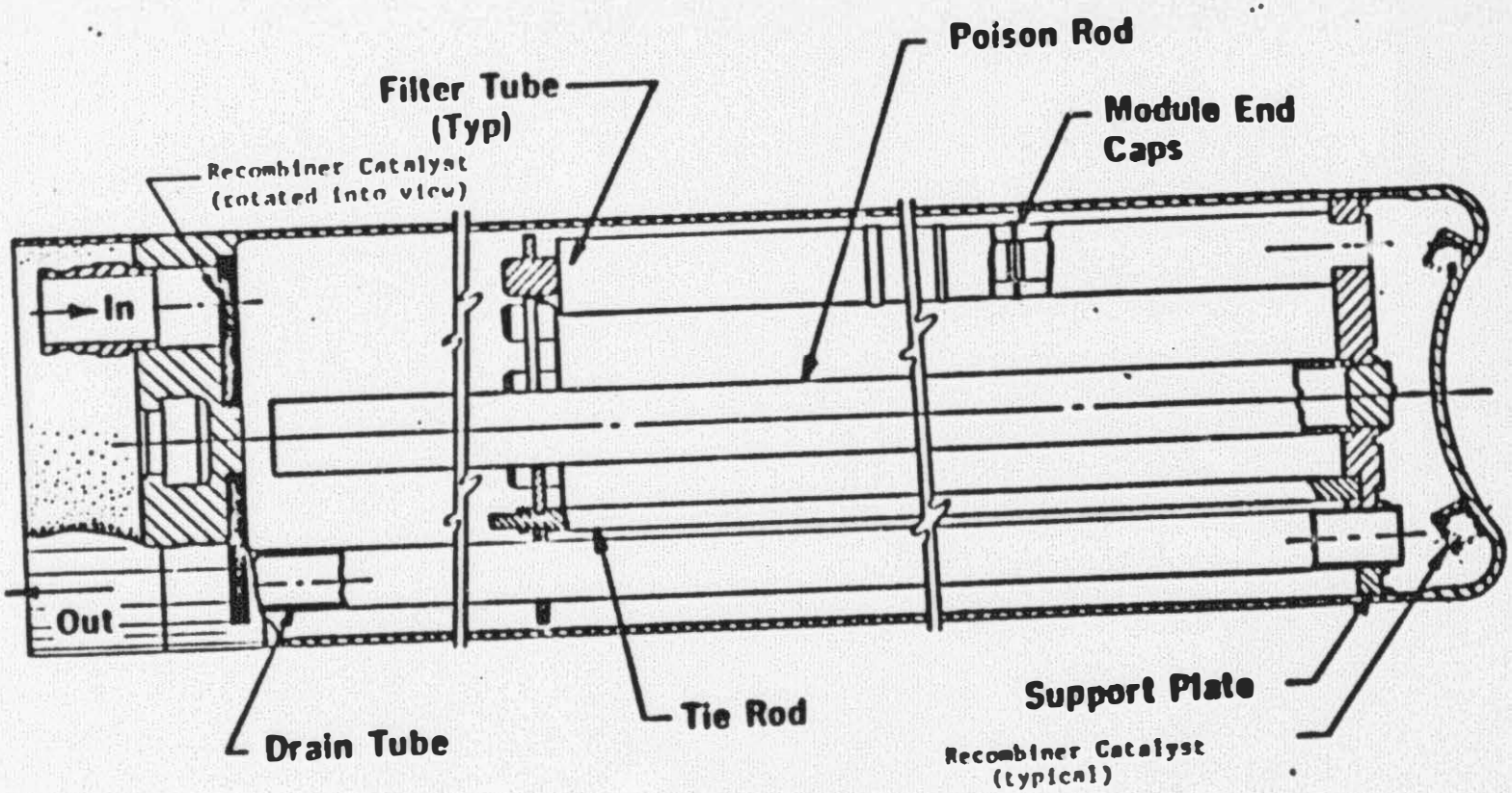

3527-016

Rev. 1

FIGURE 2.4-2

Filter Canister - Cross-Section at Mid-Plane

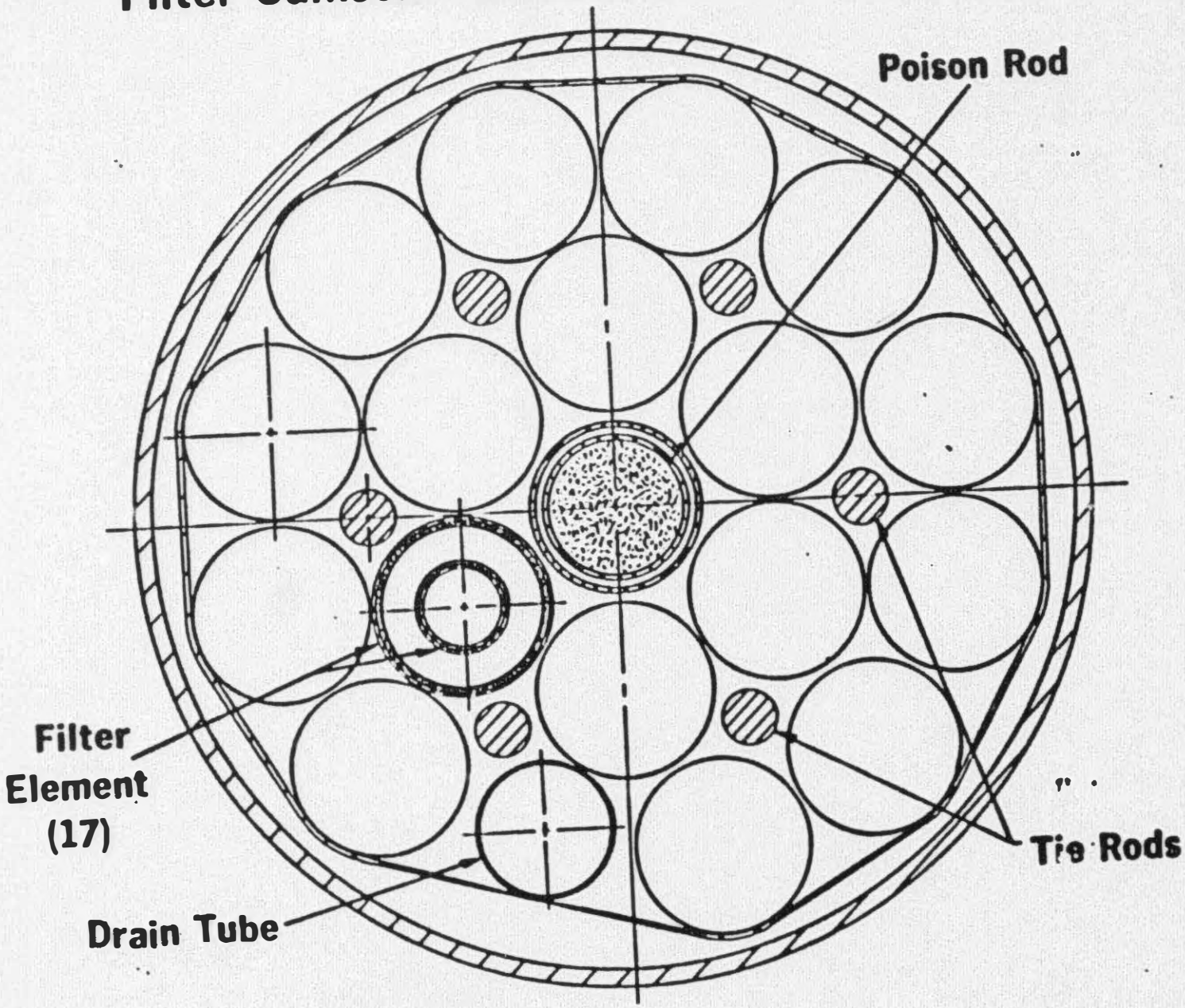

FIGURE 2.4-3

Filter Module

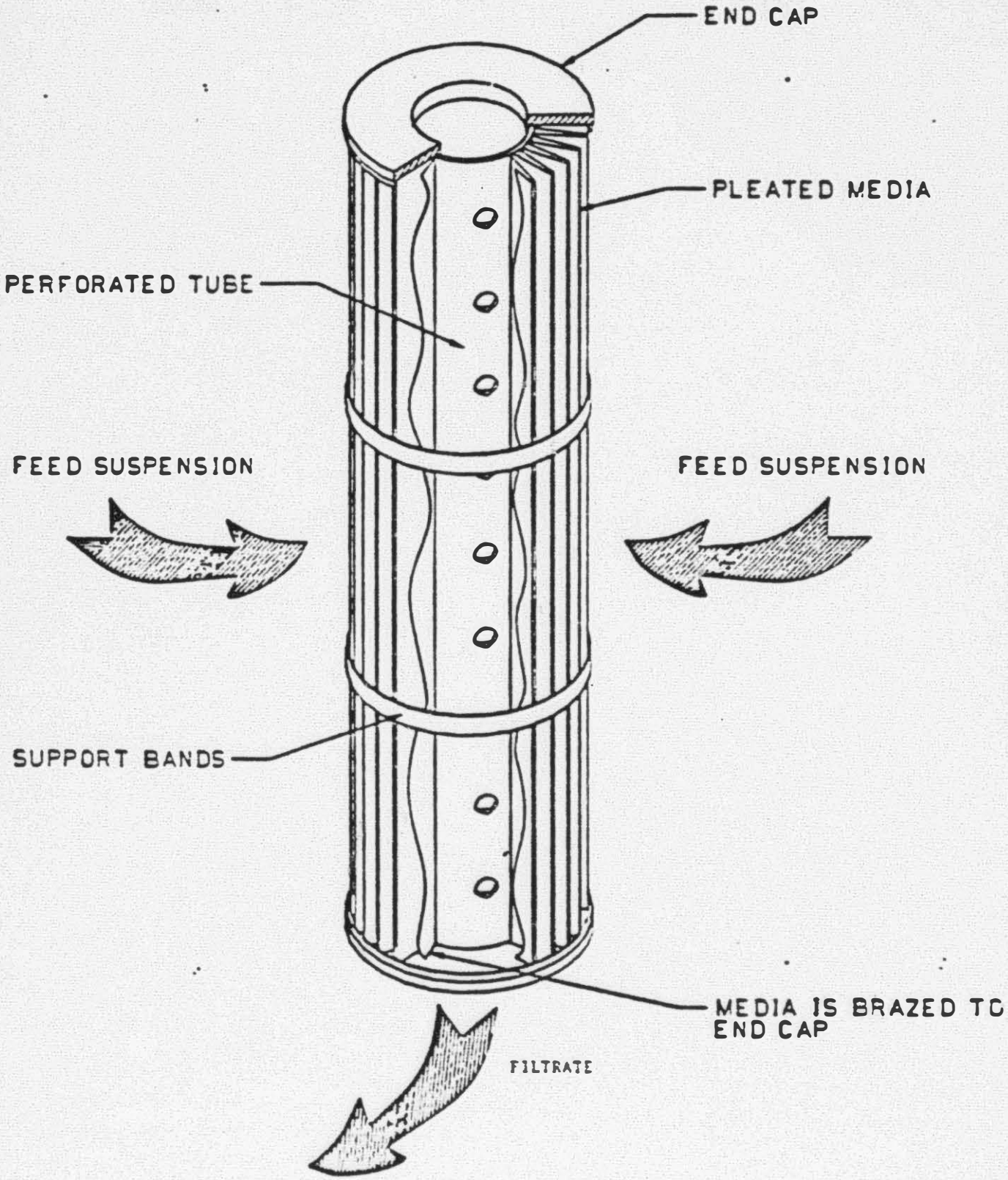

3.0 TECHNICAL EVALUATION

This section summarizes the safety issues which were evaluated during the design of the canisters. These issues deal with the expected performance of the canisters during normal operations and various design basis events. Safety issues which were evaluated include structural forces on a canister as a result of a drop accident, criticality issues associated with both single canisters and canisters in the storage racks and the canister/storage rack interface, including any constraints on the storage rack design.

3.1 Canister Structural Evaluation

A structural evaluation has been performed (Reference 1) which addresses both the loads imposed on the canister during normal operations (loading and handling) as well as postulated drops.

A combination of analytical methods and component testing is used to verify the adequacy of the design. Acceptance criteria for normal operation is based on the ASME Pressure Vessel Code, Section VIII, Part UW (lethal).

Normal operation of the canister imposes very small loads on the canister internals. The largest load on the internals is the combined weight of the debris and internals. The configuration of the canisters is such that only the lower plate assembly that supports both the debris and internals experiences any significant loads. Results of the stress analysis shows a large margin of safety for the lower plate assembly and its weld to the outer shell for all canister types. The canister shell is subject to ASME Code, Section VIII standards. Verification of the canister shell structural design to the ASME requirements has been performed (Reference 1). The canisters are designed for a combined (canister, debris, and water) static weight of 3500 pounds.

During normal handling operations (lifting), the static plus dynamic loading considered in the design of the handling features of the canister is 1.15 times the static lifted weight. Results from the structural evaluation show an acceptable margin of safety considering the stress design factors specified in NUREG-0612 and ANSI N14.6.

Normal loading of the fuel canister presents two cases for evaluation. First is the capability of the lower support plate to absorb the impact of debris accidentally dropped into the canister. Results of the dynamic impact evaluation show that the support plate can accommodate loads of up to 350 lbs (23% of a fuel assembly) dropped, in air, the full canister length without a failure of the lower plate to shell weld. This weight limit increases to 550 lbs. (in air weight) if credit is taken for the drag forces of the water in the canister. Second is the verification that placement of debris within the canister will not rupture the shroud's inner wall. This would expose the Boral sheets to the RCS water which could cause corrosion of the boral. However, examination of the shrouds subjected to drop tests (reference 10) indicate that the inner wall is resistant to debris impacts and scrapes.

A dewatering system is used to remove water from all canisters prior to shipment. During this procedure, a pressure differential is developed across the debris screen, lower support plate and drain tube. The

maximum pressure differential allowed, via a safety relief valve in the dewatering system, across canister internal components during dewatering is 55 psi. The canister internals are designed for a maximum differential pressure of 150 psi although filter media differential pressure is limited by design to 60 psid. Hence, an adequate margin of safety exists for the dewatering process.

The canisters are capable of withstanding enveloping accidents. Vertical drops of 6'-1 1/2" in air followed by 19'-6" in water, or 11'-7" in air are considered along with a combination of vertical and horizontal drops. These drops were analyzed to bound a drop in any orientation. For these cases, the structural integrity of the poison components must be maintained and the canister must remain subcritical. Deformation of the canister is acceptable. Although not expected based on the B&W drop test results, leakage of core material from the canister, up to its full contents, is allowed provided that the contents left in the canisters remain subcritical. An equivalent drop in air was calculated for the worst case and this equivalent air drop was used as the basis for the structural analysis. Structural analysis methods were used to determine the extent of the deformation of the shell and canister internals. Impact velocities were calculated for the specified canister drops. Based on these velocities, strain energy methods were used to compute the impact loads associated with the various postulated drops. Vector combinations of the horizontal and vertical components were used to determine the effect of a drop at any orientation.

In the vertical drop cases (reference 10), the same deformation will occur regardless of the canister type, since it is shell dependent. Test results from the actual canister drops have verified that for the bottom impact, all deformation occurs below the lower support plate in the lower head region. An upper bound shell deformation was computed using the ANSYS (Reference 5) computer code and the results are presented in Figure 3.1-1 along with the actual test results.

To determine the consequences of a vertical and horizontal drop on the filter and knockout canisters, their internals were analyzed with finite element methods using the ANSYS computer program. This analysis incorporated the actual non-linear properties of the material. Geometric constraints imposed by the shell were accounted for by limiting the displacement of the supports.

In the filter canister, criticality control is provided by the central B_4C poison rod coupled with the mass of steel in the filter element drain tubes and tie rods. Using the end caps of the filter modules as deflection limiters, the entire tube array deflection is limited to 1.6" under postulated accidents. This analysis is conservative because it does not take into account the 5 circumferential bands around the array or the viscosity of the filter cake bed, both of which would tend to maintain the standard spacing. Using the maximum calculated deformed geometry (before the array bounced back closer to its original position), the criticality criterion given in section 3.2 was met.

In the knockout canister, criticality control is provided by the central B_4C poison rod coupled with four absorber rods. Results from the structural analysis show that the poison rods remain essentially elastic during all postulated accidents and the maximum instantaneous displace-

ments are less than 0.75 inch. The minor modifications made to some of the knockout canisters to convert them to "deep-bed" filters (Section 2.3) are within the bounds of the values used in the analysis and testing of the knockout canisters. Thus, the "deep bed" filters are expected to exhibit similar structural behavior as the knockout canisters during a drop accident. As in the case of the filter canister, the resultant deformed geometry successfully met the criticality criterion given in section 3.2.

The fuel canisters, with their square-within-a circle geometry, exhibit different drop behavior than the other canisters. For both the vertical and side drops, the fuel canister internals will not experience significant deformations other than the shell deformations discussed above. Lightweight concrete filling the void between the square inner shroud and the circular outer shell provides continuous lateral support to both the outer shell and the shroud. This results in a distributed loading function for horizontal drops resulting in no calculated deformation to the shroud shape. Testing has demonstrated that the lower support plate remains in place for design drops while supporting a mass equal to the shroud, payload and the concrete. The lack of significant deformation after a drop (reference 10) makes the criticality analysis for the standard design applicable to the drop cases as well.

3.2 Canister Criticality Evaluation

Criticality calculations were performed to ensure that individual canisters as well as an array of canisters will remain below the established k_{eff} criterion under normal and faulted conditions. The criticality safety criterion established is that no single canister or array of canisters shall have a k_{eff} greater than 0.95 during normal handling and storage at the TMI-2 site. For plant accidents (e.g., drained spent fuel pool), the criticality safety criterion established is a $k_{eff} \leq 0.99$. These criteria are satisfied for all canister configurations.

The "deep bed" filters do not alter the placement of the poison rods in the knockout cansiters and the d.e. and/or sand added to these canisters has less moderating ability than water; thus, the criticality evaluations performed for the knockout canisters would bound the "deep-bed" filters. In addition, the criticality evaluations performed on the knockout canisters following drop accidents would bound dropped "deep-bed" filters since the structural behavior of the "deep-bed" filters is similar to the knockout canisters.

Coagulants and d.e. used in DWCS to improve filter canister performance has been evaluated in Reference 12. This evaluation has shown that the addition of these materials in the canisters would not adversely impact the criticality evaluations presented herein. Additionally, the accumulation of coagulants and d.e. in the canisters would not adversely affect the conclusions presented in Attachment 2 regarding the subcriticality of the stored canisters in a postulated dry storage pool.

The computer codes used in this work were NULIF, NITAWL, XSDRNPM and KENOIV (References 6, 7, 8 and 9). The NULIF code was used primarily for fuel optimization studies in a 111 energy group representation. NITAWL and XSDRNPM were used for processing cross sections from the 123

group AMPX master cross section library. NITAWL provides the resonance treatment and formats the cross section for use by either XSDRNPM or KENOIV. In most cases, XSDRNPM cell weighted cross sections were used in the KENOIV calculations but for some comparative fuel optimization runs the NITAWL output library was used directly by KENOIV.

The calculational models assume the following conditions for the canister contents:

1. Batch 3 fresh fuel only

2. Enrichment: batch 3 average + 2σ (highest core enrichment)

3. No cladding or core structural material

4. No soluble poison or control material from the core

5. Optimally moderated, stacked, standard whole fuel pellets

6. Canister fuel regions are completely filled without weight restrictions

7. Uniform 50°F temperature

8. B-10 surface density was assumed to be 0.040 gm/cm^2 in the Boral used for the fuel canister. (Actual B-10 surface density will be 0.040 gm/cm^2 with a 95/95% confidence level in the testing to provide at least a 2σ margin.)

9. B_4C density used is the poison tubes for the filter and knockout canister was assumed to be 1.35 gm/cm^3 with the boron weight percent assumed to be 70%. (Actual B_4C density will be at least 1.38 gm/cm^3 with a boron weight percent meeting requirements for ASTM-C-750 Type 2 B_4C powder, minimum boron weight percent 73%.)

Optimization studies were performed to determine the value of these parameters. These optimization studies are presented in Reference 1 along with other parametric studies performed for special cases.

The KENO analysis employs a fuel model that bounds all debris loading configurations. Three basic configurations were analyzed for each canister: a single canister surrounded by water, an array of canisters in the storage pool and a disrupted canister model resulting from an enveloping drop. The standard canister configuration assumed that some minimum degree of damage could have occurred in the canisters during normal loading operations. All the canisters analyzed in an array were assumed to have this minimum damage. A 17.3" center-to-center spacing was analyzed for the array cases. The 17.3" center-to-center spacing accounts for all storage rack tolerances and is the minimum center-to-center spacing possible for any two canisters. The canisters are assumed to be loaded with debris consisting of whole fuel pellets enriched to 2.98 w/o, optimally moderated with 50°F unborated water. The analysis will provide conservative results and bound any actual configuration including draining of the canisters during the dewatering operation. For accident conditions, it is assumed that optimized fuel is present in both normal fuel locations and in all void regions

internal to the canister. Filling all void regions with fuel has the effect of adding fuel to the canister after a drop.

The canister shell, including the lower head, is identical for all three canisters. The cylindrical shell is modeled using the maximum shell OD of 14.093" and the nominal 0.25" wall thickness. The model explicitly describes the concave inner surface but squares off the rounded corners. This increases the volume of the lower head.

All three canisters contain catalytic material for hydrogen recombination in both the lower and upper head. This material and its structural supports are not included in the models. The volume occupied by these materials is replaced with fuel. In addition, the protective skirt and nozzles on the upper canister head are not modeled.

The storage rack cases assume the canisters are stored in unborated water with a 17.3" minimum center-to-center spacing. Sensitivity studies were performed on the nominal 18" center to center spacing to determine the effect of a canister dropped outside of the rack. These analysis show that k_{eff} <0.95 for canisters dropped outside the rack as long as the side of the dropped canister does not come within 2" of the side of the nearest canister in the rack. This requirement is met by the storage rack design (Reference 2).

Three cases are examined for a dropped canister: a vertical drop, a horizontal drop and a combined vertical and horizontal drop. The shell deformation is essentially the same for all cases. For these drops, the cylindrical shell is assumed not to deform. Any deviation from the cylindrical shape would increase the surface to volume ratio and increase the neutron leakage from the system. In the lower head region of the shell, a tear drop shape expansion is assumed to occur. The bottom head is modeled as a flat plate with the internal components resting on it. To bound all drop cases, the canister was assumed to rotate during a drop and land on its head. A similar tear drop shape will result. Both of these cases were merged into a single model that assumes the tear drop deformation at both the top and bottom with the internals displaced to the flattened lower head surface. For the combined vertical-horizontal drop, the radial displacement of the internal components is combined with the double tear drop model. This drop model bounds any conceivable drop configuration by exceeding conservative stress estimates of deformation.

Results

The results of KENO, using basic three dimensional canister models are presented in Table 3-1. These results represent bounding values for any configuration of the canisters at TMI-2.

Basically, they show that for any configuration, the effective multiplication factor, with uncertainties included, will be less than 0.95. Due to the conservatism built into the models, the k_{eff} of any actual configuration will be less than these bounding values.

Three assumptions used in the analyses reported in Table 3-1 have been reevaluated. The affected assumptions are:

1. type of poison used in the filter and knockout canisters,

2. storage pool water temperature, and

3. fuel particle size.

The values reported in Table 3-1 for the filter and knockout canisters are based on the assumption that the poison tubes for the canisters are filled with vibrapacked B_4C powder. Actual fabricated filter and knockout canisters contain compressed sintered B_4C pellets. This change resulted in a small reduction to the diameter of the poison in the canisters which results in a small increase in the multiplication value (k_{eff}) of the two canister types. Based on analyses the increase in multiplication will not exceed 0.4% Δk.

The values reported in Table 3-1 assume a minimum temperature of 50°F for all canister types. For canisters stored in the spent fuel pool the temperature could be as low as 32°F. Explicit criticality array calculations were not performed at this lower temperature. Rather, an evaluation was performed to determine the maximum increase in multiplication due to cooling from 50°F to 32°F. The maximum change in multiplication was determined to be an increase of 0.1% Δk.

The results reported in Table 3-1 are also based on the assumption that no single fuel mass greater than a whole fuel pellet exists in the TMI-2 core. Examinations of the core have indicated that fuel melting may have occurred. To assess the impact of this possibility, an evaluation was performed to determine the k_∞ for the most reactive batch 3 fuel particle size. The k_∞ for the optimum size particle was only 0.07% Δk higher than the k_∞ for the standard whole pellet. The corresponding increase in k_{eff} would be approximately the same magnitude. Thus, there is no limit on the sizes of fuel particles that can be placed in the fuel and knockout canisters.

In conclusion, the changes in k_{eff} resulting from the three modified assumptions will not result in exceeding the k_{eff} criterion of 0.95 for the cases reported in Table 3-1.

3.3 Canister Hydrogen Control Evaluation

A generic feature of the canisters is the recombiner catalyst package incorporated into the upper and lower heads of all the canisters. The catalyst recombines the hydrogen and oxygen gases formed by radiolytic decomposition of the water trapped in the damp debris. This reduces the buildup of internal pressure in the canister and keeps the gases below the flammability limit. The redundant locations ensure that a sufficient quantity of catalyst is available for any canister orientation in which hydrogen might be generated (e.g., an accident which leaves a canister upside down). Test results (Reference 4) have shown that the catalyst will perform effectively when dripping wet, but not when submerged.

A single catalyst bed, which contains at least 100 grams of catalyst, is incorporated in the upper heads of the fuel canisters. Two catalyst beds, each containing at least 50 grams of catalyst, are incorporated in the upper heads of the filter and knockout canisters. Four catalyst beds, each containing at least 25 grams of catlayst, are installed in

the lower heads of all the canisters. Thus, each canister contains at least 200 grams of catalyst. The catalyst beds were designed to meet the shape and volume requirements established from testing by RHO (Reference 4).

Canister dewatering in the FHB will ensure that a sufficient quantity of catalyst would be exposed (not submerged in water) in a dewatered canister in any orientation. This sufficient quantity of catalyst will be 50% more catalyst than required. The required quantity of catalyst is determined by catalyst testing that considers catalyst contaminations which may occur during canister fabrication and loading and chemical additions to improve DWCS filter performance and to control microbiological growth in the RCS. Reference 13 provides a detailed evaluation on canister dewatering criteria in order to expose a sufficient quantity of catalyst to achieve a minimum safety factor of 1.5.

The maximum predicted gas generation rate in a canister has been determined by two separate models: (1) the maximum theoretical gas generation rate and (2) the maximum realistic gas generation rate. The maximum theoretical gas generation rate was determined by Rockwell Hanford Operations (RHO) in their document RHO-WM-EV-7 (GEND-051) for purpose of developing the catalytic recombiner bed design. The maximum realistic gas generation rates were determined by GPU for purposes of predicting canister internal pressures during periods when the canisters are water solid.

Both models are based on the Turner paper, "Radiolytic Decomposition of Water in Water-Moderated Reactors Under Accident Conditions", referenced in the RHO report. The basic relationship is:

$H_2 = (W)(F)(G)(r)\ 8.4 \times 10^{-3}$ liters/hour

where:
F = fraction of β and γ energy absorbed in water
G = H_2 generation value in moles/100 eV
r = ratio of peak to average decay heat energy in the fuel debris
W = ionizing radiation per canister (watts)
8.4×10^{-3} = unit conversions (L ev/W.hr)

For the maximum theoretical generation, the above factors are maximized as follows:

- o W - the maximum quantity of fuel debris in any canister, not including residual water weight or weighing accuracy, is assumed. (W = 54.2)
- o F - The fraction of β and γ energy absorbed is conservatively high and large amounts of water are also assumed to be available for absorbtion which is in excess of what is possible in the canisters. (F = 0.2)
- o G - The hydrogen gas generation value is based on a) completely turbulent/boiling conditions when the radiolytic gases are instantly removed from the generation site and b) no build up of hydrogen overpressure which tends to retard radiolysis. (G = 0.44)

- o r - The ratio of peak-to-average decay heat energy in the fuel is based on the most active region of an undamaged core. This assumes the fuel is intact and not scattered to other regions. (r = 1.9)

For the maximum realistic generation of hydrogen and oxygen, the worst case realistic factors for the damaged TMI core are used as follows:

- o W - The maximum quantity of fuel debris expected in any canister is used which includes allowances for residual water and weighing accuracy. (W = 50)

- o F - The fraction of ß and γ energy absorbed is based on the maximum amount of water possible in an actual canister. (F = 0.07)

- o G - The hydrogen gas generation value is based on the actual worst case core debris conditions expected in a canister which includes lower temperature, quiescent conditions. (G = 0.12)

- o r - The ratio of peak to average decay heat energy in the fuel debris is based on the worst case conditions in the damaged TMI core. (r = 1.4)

The resulting hydrogen/oxygen generation rates for the two models are:

	Max. Theoretical liter/hour	Max. Realistic liter/hour
H_2	7.6×10^{-2}	5.0×10^{-3}
O_2	3.8×10^{-2}	2.5×10^{-3}
Total	1.14×10^{-1}	7.5×10^{-3}

The generation of other gases was not considered. Since the amount of contaminants in the RCS is small, the generation of other gases from the radiolytic decomposition of these contaminants is not expected to be significant.

Using the maximum realistic gas generation rate of 0.0075 liters/hour and assuming no recombination or scavenging of oxygen, the 25 psig relief valve is estimated to first open in approximately 25 days for the worst case canister. Released gas will be vented through the pool water directly to the containment or fuel handling building and is such a small quantity that it will cause no combustion concerns in the atmosphere of these buildings.

To address the issue of canister pressurization resulting from failure of the 25 psig relief valve a second relief valve is installed on the canisters. This relief valve will ensure that canister pressure does not exceed the design limit of 150 psig. The additional relief valve will make the canister single failure proof with regards to pressurization. This second valve will also be installed in such a manner to eliminate common mode failure of the two pressure relief valves.

The recombiner catalyst is ineffective when it is under water. An evaluation has been performed to determine how long it takes an undewatered canister to reach 150 psig if the 25 psig relief valve fails closed. This time for the worst case canister is 139 days. A similar concern exists for the dewatered canister should a signficant amount of oxygen scavenging occur and the 25 psig relief valve fails closed. Assuming no recombination, (i.e. complete oxygen

scavenging) the canister will reach the design pressure in 2362 days for a fully loaded fuel canister with 25% void volume following dewatering.

If the relief valve should fail open while the canisters are being stored there is the possibility that fuel debris can be released into the pool water. If contaminants are released into the pool the defueling water cleanup system (DWCS) can be used as necessary to limit the contamination level of the water. Hence, a failed open relief valve does not pose a safety concern. Additionally, given that it is planned, although not required, to dewater the canisters shortly after they are loaded, pressurization of the canisters caused by hydrogen/oxygen generation will be minimal and the relief valve is not expected to open.

Although not considered a credible event, the consequences of a hydrogen ignition inside a canister has been evaluated. The maximum pressure that can be reached inside a canister under normal conditions, because of the 25 psig relief valve, is approximately 42 psia. This pressure includes the 25 psig set pressure and 5 feet of water submergence. Under the assumption that the recombiner catalyst does not function properly, a flammable mixture of hydrogen and oxygen can accumulate within a canister. If an ignition of this mixture is postulated, an overpressurization of the canister could occur. The ultimate stresses will be reached for various canister components at the estimated pressures:

- canister shell - 2160 psi
- fuel canister bolts - 2900 psi
- threaded connections - 2500 psi

Considering the large margin that exists between these pressures and the maximum, normal condition canister pressure (i.e., approximately a factor of 50), the overpressurization resulting from an ignition of hydrogen within the canister is not expected to affect the overall canister integrity.

TABLE 3-1

Results of 3D KENO Criticality Calculation

Description	$k_{eff}+2\sigma$	Histories	Maximum k_{eff}*
Filter Canister**			
Single, Ruptured Filters	0.795 ± 0.024	9331	0.839
17.3" Array, Ruptured Filters	0.823 ± 0.021	52374	0.867
Vertical Drop, Ruptured, without filter screens	0.798 ± 0.025	8127	0.843
Horizontal Drop, Ruptured, without screens	0.843 ± 0.010	15050	0.873
Combined Horizontal/Vertical Drop, Ruptured, without screens	0.851 ± 0.021	44869	0.892
Fuel Canister			
Single, Standard Configuration	0.825 ± 0.012	15050	0.857
17.3" Array, Standard Configuration	0.829 ± 0.025	6321	0.877
Knockout Canister**			
Single, Standard Configuration	0.835 ± 0.018	10535	0.873
17.3" Array, Standard Configuration	0.877 ± 0.015	11438	0.915
Vertical Drop, Single	0.843 ± 0.019	9933	0.882
Horizontal Drop, Single	0.853 ± 0.008	26488	0.881
Combined Horizontal/Vertical Drop, Single	0.851 ± 0.016	12943	0.887

*$k_{eff} + 2\sigma$ + calculational bias (see Reference 1)

**results are based on vibrapacked B_4C powder in the poison tubes

FIGURE 3.1-1

SHELL DEFORMATIONS - VERTICAL DROP (ALL CANISTERS)

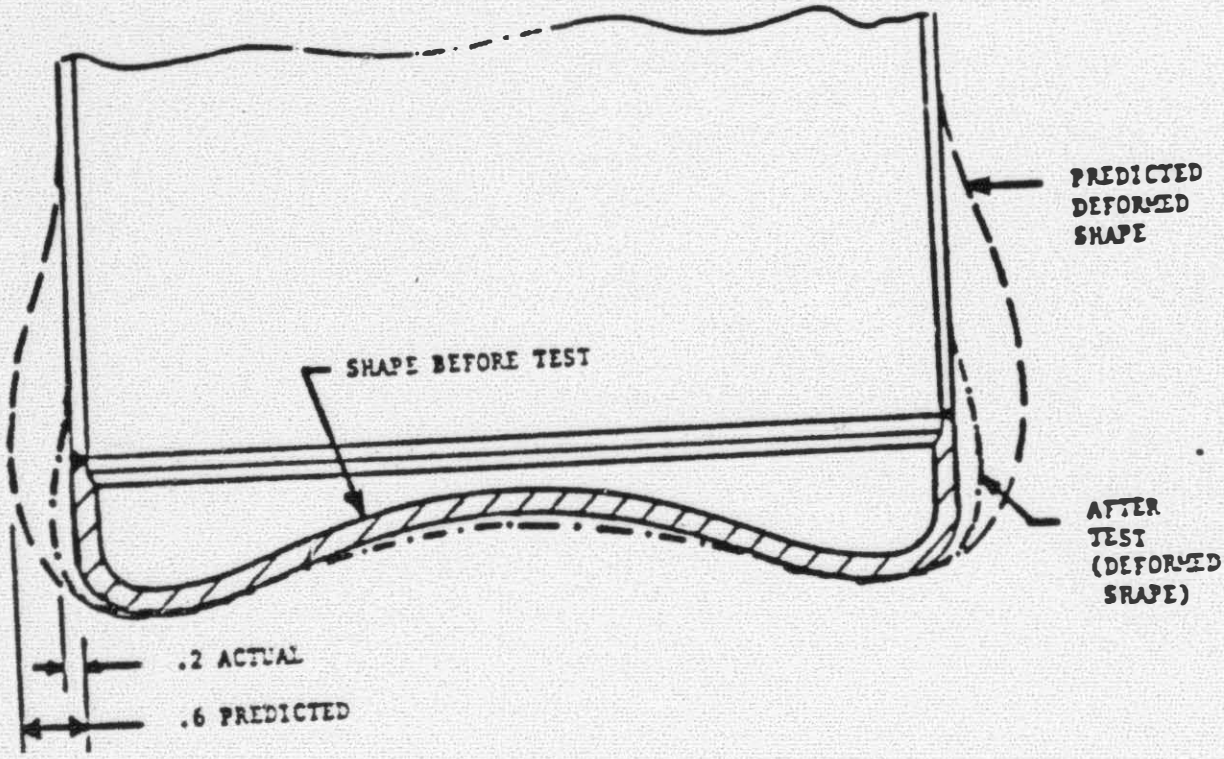

4.0 RADIOLOGICAL CONSIDERATIONS

The canisters are designed to be loaded with core debris from the TMI-2 RCS. These canisters do not contain internal shielding and must be shielded during all handling and storage operations.

The shielding requirements for the various canister operations (e.g. loading, handling, and storage) are discussed in reference 3.

Personnel exposure from the loaded canisters will be addressed in Reference 3 as part of the canister handling sequence.

5.0 10 CFR 50.59 EVALUATION

Changes, Tests and Experiments, 10 CFR 50, paragraph 50.59, permits the holder of an operating license to make changes to the facility or perform a test or experiment, provided the change, test or experiment is determined not to be an unreviewed safety question and does not involve a modification of the plant technical specifications. A proposed change involves an unreviewed safety question if:

a. The probability of occurrence or the consequences of an accident or malfunction of equipment important to safety previously evaluated in the safety analysis report may be increased; or

b. the possibility for an accident or malfunction of a different type than any evaluated previously in the safety analysis report may be created; or

c. the margin of safety, as defined in the basis for any technical specification, is reduced.

The defueling canisters replace the fuel cladding lost during the accident as the barrier for containing the fuel. As discussed in Section 1.1 of this TER, the purpose of this evaluation is to show that the canisters are designed to remain safe under normal operation and handling conditions as well as postulated drop accidents and storage. The scope of the evaluation relates only to design aspects and not in field canister use which is addressed in the Safety Evaluation Report for Early Defueling of the TMI-2 Reactor Vessel (Reference 3). On this basis the scope of this 10 CFR 50.59 Evaluation is limited to design aspects of the canister.

The issues of concern with canister design are criticality control and overpressurization protection. With respect to criticality control, this evaluation shows that the canister will remain subcritical under any configuration or following structural deformation due to a load drop. With respect to overpressurization protection, two relief valves will be installed on each canister to prevent the possibility of a single failure or common mode failure from overpressurizing the canister. Thus, it can be concluded that the design of the defueling canisters neither increases the probability of any accident previously evaluated nor creates the possibility of a different type of accident. Additionally, as the current TMI-2 Technical Specifications do not specifically address containment of the fuel debris, the margin of safety as defined in the basis of the Technical Specifications is not reduced.

As discussed above, these canisters are critically safe by design. Additionally, activities associated with canister closure and handling, including

installation of the relief devices, will be performed in accordance with procedures prepared, reviewed and approved in accordance with TMI-2 Technical Specifications Section 6.8, which requires NRC approval of certain types of procedures. Therefore, as no further engineering controls are needed to ensure criticality safety and activities associated with canister closure and handling will be controlled in accordance with procedures subject to Technical Specification Section 6.8, it is GPU Nuclear's belief that no changes to the Technical Specifications are required.

In conclusion, within the bounds described in this report, the design and use of the defueling canisters do not result in an unreviewed safety question, nor require changes to the TMI-2 Technical Specifications.

6.0 CONCLUSION

Canisters are needed to provide effective long term storage for the TMI-2 core debris. Three types of canisters are required to support the defueling system: fuel, filter and knockout canisters. These canisters have been evaluated to determine if they could safely perform their function under normal and accident conditions. The results of this evaluation show that the canisters will remain subcritical under normal operations, handling and accident conditions. A structural evaluation of the canisters has shown that they maintain their integrity and will function as designed under normal operating conditions. Drop analyses and drop tests were used to determine the effect of a design basis drop on the canister shell and internals. The results from these analyses were used in determining the reactivity of the canisters under accident conditions. Therefore, based on structural and criticality considerations, it can be concluded that these canisters can safely function under normal and accident conditions at TMI-2.

7.0 REFERENCES

1. TMI-2 Defueling Canisters Final Design Technical Report, Babcock and Wilcox, Document No. 77-1153937-05, dated March 28, 1986.

2. Technical Evaluation Report for Fuel Canister Storage Racks, 3253-012, Revision 1.

3. Safety Evaluation Report for Defueling of the TMI-2 Reactor Vessel, 4350-3261-85-1, Revision 1.

4. Evaluation of Special Safety Issues Associated with Handling the TMI-2 Core Debris, RHO-WM-EV-7, Rockwell Hanford Operations, February 1985.

5. Computer Code "ANSYS", Revision 4.1, March 1, 1983, Swanson Analysis System Inc., Houston, PA.

6. "NULIF-Neutron Spectrum Generator, Few Group Constant Calculator and Fuel Depletion Code", BAW-426, Revision 5.

7. "NITAWL, Nordheim Integral Treatment and Working Library Production," NPGD-TM-505.

8. "XSDRNPM AMPX Module with One Dimensional S_n Capability for Spatial Weighting," AMPX-II, RSIC-RSP-63, ORNL.

9. "KENO4, An Improved Monte Carlo Criticality Program," NPGD-TM-503, Revision B.

10. TMI-2 Drop Testing of Defueling Canisters Final Report, Babcock and Wilcox, Document No. 77-1156372-00, February 1985.

11. TMI-2 Early Defueling Fines/Debris Vacuum System Proof-of-Principle Test Report, TMI-AD-84-018, Westinghouse Electric Corporation, Advanced Energy Systems Division, October 1984.

12. Criticality Safety Evaluation for Coagulants, GPU Nuclear letter 4410-87-L-0021, dated February 20, 1987.

13. Safety Evaluation Report for Canister Handling and Preparation for Shipment, 4350-3256-85-1, Revision 4.

ATTACHMENT 1

TMI-2 TRANSFER SYSTEM CRITICALITY TECHNICAL REPORT

The results of this analysis are based on the assumption that the most reactive fuel particle capable of being in the knockout canister is an optimally moderated standard, whole fuel pellet. With the change to the vacuum system that permits fuel particles greater in size than whole pellets to be loaded into a knockout canister, this assumption is no longer appropriate. To assess the impact of this assumption, an evaluation was performed to determine k_∞ for the most reactive batch 3 fuel particle, when optimally moderated with unborated water. The k_∞ for the optimum size was found to be only 0.07%Δk higher than the k_∞ for the standard whole pellet. Since this increase is small and the other assumptions included in the analysis are conservative, tending to increase k_{eff}, the results presented in this attachment are still considered appropriate. Additionally, even with an increase of 0.07%Δk, the k_{eff} criterion for the canisters within the CTS will still be achieved.

TMI-2 TRANSFER SYSTEM

CRITICALITY TECHNICAL REPORT

Document No. 77-1155739-02

Published June 19, 1985

Babcock & Wilcox Company

Nuclear Power Division

Lynchburg, Virginia

Prepared for

GPU Nuclear Corporation

Under Master Services Contract 665-3212

TMI-2 Transfer System
Criticality Technical Report

Prepared by: P L. Holman — 6/19/85
P. L. Holman, Principal Engr., B&W — Date

Approved by: W G Pettus — 6-19-85
W. G. Pettus, Advisory Engineer, B&W — Date

Approved by: P C Childress — 6-19-85
P. C. Childress, Project Manager, B&W — Date

TABLE OF CONTENTS

SECTION		PAGE
1.0	ABSTRACT	6
2.0	INTRODUCTION	6
3.0	TRANSFER SHIELD AND CASK CRITICALITY ANALYSIS	7
3.1	Background	7
3.2	Scope of Calculations	7
3.3	Reactivity Criterion	7
3.4	Calculational Assumptions	7
3.5	Dancoff Factor Assumptions	15
3.6	Computer Codes and Cross Sections	15
3.7	KENIOV Bias	15
3.8	Fuel Optimization for Lead Shielded Canisters	15
3.9	Canister-Shield Gap Criticality Analysis	18
3.10	Transfer Shield Water Reflector Analysis	20
3.11	OFF-Centered Canister in Transfer Shield	23
3.12	Canister Optimization in Transfer Shield	26
3.13	Canister Insertion Analysis	29
3.14	Transfer Cask Analysis	38
4.0	CONCLUSIONS	41
5.0	REFERENCES	42

LIST OF TABLES

TABLE NUMBER		PAGE
1.	Comparison of KENOIV and XSDRNPM Results for Simple Cell Types With and Without Lead and No Poison Rods	17
2.	XSDRNPM K-effective Results for Canister-Shield Gap Analysis	19
3.	XSDRNPM Water Reflector Analysis	22
4.	XSDRNPM K-effective Results for Off-Centered Canister	25
5.	Canister-Transfer Shield Optimization Results	28
6.	Knockout Canister Insertion Study K-effective Results	33
7.	XSDRNPM Steel Liner Analysis	36
8.	K-effective for the Ruptured Knockout Canister in the Transfer Cask	40

LIST OF FIGURES

FIGURE NUMBER		PAGE
1.	Revision 1 Transfer Shield Model	11
2.	Revision 2 Transfer Shield Model	12
3.	Transfer Shield Wall Cross-Section	13
4.	Transfer Cask Model	14
5.	Off-Centered Canister XSDRNPM Model	24
6.	Typical Ruptured Knockout Canister Insertion Levels in Transfer Shield	31
7.	Reactivity Dependence of Knockout Canister Insertion Into Transfer Shield	35

1.0 ABSTRACT

The TMI-2 defueling canisters will be transferred to locations within the Reactor and Fuel Handling Buildings using a transfer shield containing lead. Transfer of canisters to the shipping cask will utilize a different device called a transfer cask. This report examines K-effective for both the transfer shield cask, with dimensions supplied by GPU Nuclear. The enclosed results indicate that for ruptured and non-ruptured canisters no poison materials other than those contained in the canisters are required in the design of either the transfer shield or cask to maintain K-effective <.95. Canisters with extensive internal damage and/or external damage from being dropped or deformed are not addressed since these canisters will be handled by GPU Nuclear on a case by case basis and are, therefore, not included in the current workscope.

2.0 INTRODUCTION

Transfer of the fuel, filter, and knockout canister designs within the Reactor Building (RB) and Fuel Handling Building (FHB) is accomplished in part using the transfer shield and transfer cask. The function of the transfer shield is to allow safe removal and transfer of canisters out of containment for reactor defueling. The transfer shield will facilitate loading the canisters into the transfer basket for movement to the FHB. A second transfer shield will be located within the fuel handling facility for the placement of canisters within the storage racks, subsequent transfer to a dewatering station, and transfer of canisters to a transfer cask loading station. A transfer cask will be located within the FHB to allow movement of debris filled canisters into shipping casks.

From the description provided in Reference 1 by GPU Nuclear the transfer shield comprises a long hollow cylindrical lead shield. The inside and outside of the lead shield will be lined with steel for structural support. A smaller movable outer lead shield will be lowered at least one foot below the water surface prior to withdrawal of the canister into the transfer shield. This outer shield can be raised once the canister is fully inserted to allow clearance of the shield from obstructions. The shorter length outer shields will also be lined with steel for structural support. The transfer shield will be attached to a canister handling trolly to allow transfer of the canisters within the shield as a unit. The canisters will be withdrawn into the transfer shield by a canister grapple and cables connected to a hoist which is mounted on the movable trolly.

The transfer cask is similar to the transfer shield with the main walls of the transfer cask containing 4.5 inches of lead with 1 inch inner and outer steel linings for structural support. The transfer cask has a movable bottom door to allow insertion of a canister by a grapple and cable mechanism and subsequent closure of the cask upon canister insertion. Located below the bottom door is a lead/steel-lined flange that projects outward from the cask to reduce levels of backscattered radiation. The hoist for the transfer cask is located to one side of the cask and near the cask midplane. The entire transfer cask is suspended by a crane.

3.0 TRANSFER SHIELD AND CASK CRITICALITY ANALYSIS

3.1 Background

The criticality studies in this report have proceeded at times in parallel or in advance of normally required mechanical design information. Where specific dimensions on the transfer cask or shield were available they, were incorporated into the analysis. In some cases information was not available and dimensions were chosed in a fasion to produce a bounding analysis and maintain conservatism. For further details see the section on assumptions.

Calculations in this report address the following objectives: 1) evaluate the optimal fuel composition with the lead shield in place, 2) determine the effect of the gap region between the inserted canister and the cask or shield for centered and off-centered canisters, 3) determine the most reactive canister type in the transfer shield, and 5) evaluate the most reactive canister for the worst insertion point in the transfer cask. Canister criticality results for both ruptured and non-ruptured as well as single and lattice configurations are summarized in recent technical reports.[2,3]

3.2 Scope of Calculations

The required scope of criticality calculations is detailed in the "Technical Specifications for Design of Defueling Canisters for GPU Nuclear Corporation Three Mile Island Unit 2 - Nuclear Power Plant" Appendix E, Section 1.2.[4] Section 1.2.3 specifically details transfer criticality, although subsequent changes to the work scope were negotiated.

3.3 Reactivity Criterion

The reactivity criterion for criticality safety used in this analysis is that the value of K-effective for the most reactor canister inside the transfer system shall not exceed 0.95. These analysis are consistent with 10 CFR 72.73 and ANSI/ANS 8.1, 8.17, and 16.5[5,6,7,8] within the workscope negotiated by GPU Nuclear.

3.4 Calculational Assumptions

The calculational models for the canisters[2,3] in the transfer shield or cask assume the following conservative conditions.

1. Batch 3 unirradiated fresh fuel only.

2. Enrichment: batch 3 average + 2σ (2.98 wt% U-235).

3. No cladding or core structural material.

4. No soluble poison or control materials from the reactor core.

5. Optimal fuel lump size and volume fraction and optimal water moderator density (except in parametric cases for the optimization study).

6. Canister fuel regions completely filled without weight restriction. If a weight restriction were to apply and canisters were partially filled with clean water or structure the result would be lower canister reactivity.[3].

7. At leasts 2σ allowance in fixed poison concentrations.

8. Uniform 50°F temperature.

9. Infinite media Dancoff factors (see Dancoff Factor Assumptions).

The model for the transfer shield assumes the following conditions (see Figure 1 for Revision 1 model and Figure 2 for Revision 2 model).

1. The trolly was modeled as a 4x4 foot, 12 inch thick block of steel. This assumption will be conservative since steel in air will be a good reflector of epithermal neutrons.

2. A movable horizontal lead shield 15.5 inches in diameter is assumed to be 6 inches and located 20 inches from the top of the upper canister head at all canister insertion levels. Because of the conservative size of this lead shield, the grapple was not specifically modeled.

3. The shield walls were originally assumed to be made entirely of lead for the transfer shield to provide maximum reflection without absorption or removal of epithermal neutrons. This assumption applies to all transfer shield cases originally contained in Revision 1 of this document. For Revision 2 calculations, the steel liners are explicitly modeled.

4. For Revision 1 calculations, the lead walls were assumed to be 5.125 inches thick which includes the 0.125 inch air gap modeled as being lead filled for conservatism. Additionally, the inside diameter of the walls are 15.5 inches and extend the entire length of the transfer shield. Revision 2 analyses assume an inner shield wall that extends the full length of the transfer shield with a combined steel and lead thickness of 3-7/32 inches. The inner full length shield is followed by an 11/64 inch air gap and a 9 ft. long movable outer shield. The 9 ft. long movable outer shield has a combined lead and steel thickness of 2-5/32 inches. Attached to the movable outer 9 ft. shield is a shorter 30 inch long shield with a lead and steel thickness of 2-61/64 inches. These dimensions yield a maximum lead and steel thickness less the air gap of 8-21/64 inches at the base and a minimum thickness of 3-7/32 inches above the 9 ft. long outer shield. The inside diameter of the transfer shield is 15-5/8 inches. Shown in Figure 3 is a cross-sectional cut of the transfer shield wall with lead and steel dimensions.

5. For Revision 1 calculations, the water level of the pool is level with the bottom of the transfer shield since lead with an air gap between the canister and shield was shown to be more reactive than lead with a water gap (see canister shield gap analysis). In Revision 2 analyses, the canister shield gap was air filled as before but water was modeled for a length of 2 ft. outside the

shield to maximize reflected neutrons to the canister. This modification was shown with XSDRNPM to be conservative (see Section 3.10 - Transfer Shield Water Reflector Analysis).

6. Dry air is modeled in the region between the canister and shield and in regions external to the shield. This will minimize thermalization of reflected neutrons and reduce subsequent absorption in non-fissioning structural material. Dry air is assumed to consist of pure oxygen will have a negligible effect on k-effective considering the small density of air even for the 20 inch vertical gap between the top of the canister and lead shield. There are three orders of magnitude difference between the density of air and a material like water. Furthermore, results of the canister shield gap analysis (see Section 3.9.2) shows a trend that indicates the most reactive material for the gap region that could be assumed is void. Finally, since the top and bottom heads of the canister are low importance and low fission density regions the effect of the assumed composition of air in this region is insignificant on calculated results with a published code like KENOIV.

7. Although there is an air gap between the bottom of the transfer shield and the water level when the outer shield is raised, this gap is not modeled to prevent neutron streaming.

8. No soluble boron is assumed in any water regions.

9. For the canister types examined, only internally ruptured configurations due to filter screen failure were examined in the transfer shield since these are most reactive.[2,3]

10. The upper head protective skirt on the canisters is not modeled.

11. The transfer shield in Revision 2 calculations models the latest knockout canister geometry with shorter B_4C rods.

The model for the transfer cask assumes the following (see Figure 4).

1. No trolly is modeled since the transfer cask is supported by a crane.

2. A horizontal lead shield 15 inches in diameter is assumed to be 6 inches thick and located 10 inches from the top of the upper canister head. Because of the conservative size of this lead shield, the grapple was not specifically modeled.

3. The 15 foot 1 inch long upper lead shield is assumed to have 4.5 inches of lead with a 1 inch steel liner on all sides. The inside diameter of the main shield is 15 inches.

4. The bottom lead door is assumed to be 4 inches thick with 0.5 inches of steel liner on all sides. The diameter of the bottom door is conservatively extended to 43 inches in Revision 2 analyses.

5. The lead/steel flange located below the bottom door projects 7.5 inches radially beyond the main cask walls. This flange is 4 inches thick with a 0.5 inch liner on all sides. The radial width of the flange is 14 inches.

6. The region below the 4 inch thick lead-door was filled with lead for conservatism in Revision 2 calculations. This gives a combined lead and steel thickness below the canister of 10 inches.

7. A lower shield collar (loading boot) is assumed to be 3 ft. long, with a thickness of 3 inches of lead and 1 inch of steel liner on all sides. Although the loading boot is no longer required, it is retained for conservatism.

8. The loading boot extends 2 ft. long below the water surface.

9. Dry air is modeled in the gap region between the canister and cask and in regions above the water surface external to the cask.

10. No soluble boron is assumed in any water regions.

11. Only internally ruptured canister configurations due to screen failure were considered since these are most reactive.[3]

12. The protective skirt on the canisters are not modeled.

13. The transfer cask models the knockout canister with the latest geometry and shorter B_4C rods in Revision 2 analyses.

6. The region below the 4 inch thick lead-door was filled with lead for conservatism in Revision 2 calculations. This gives a combined lead and steel thickness below the canister of 10 inches.

7. A lower shield collar (loading boot) is assumed to be 3 ft. long, with a thickness of 3 inches of lead and 1 inch of steel liner on all sides. Although the loading boot is no longer required, it is retained for conservatism.

8. The loading boot extends 2 ft. long below the water surface.

9. Dry air is modeled in the gap region between the canister and cask and in regions above the water surface external to the cask.

10. No soluble boron is assumed in any water regions.

11. Only internally ruptured canister configurations due to screen failure were considered since these are most reactive.[3]

12. The protective skirt on the canisters are not modeled.

13. The transfer cask models the knockout canister with the latest geometry and shorter B_4C rods in Revision 2 analyses.

Figure 1

Revision 1 Transfer Shield Model

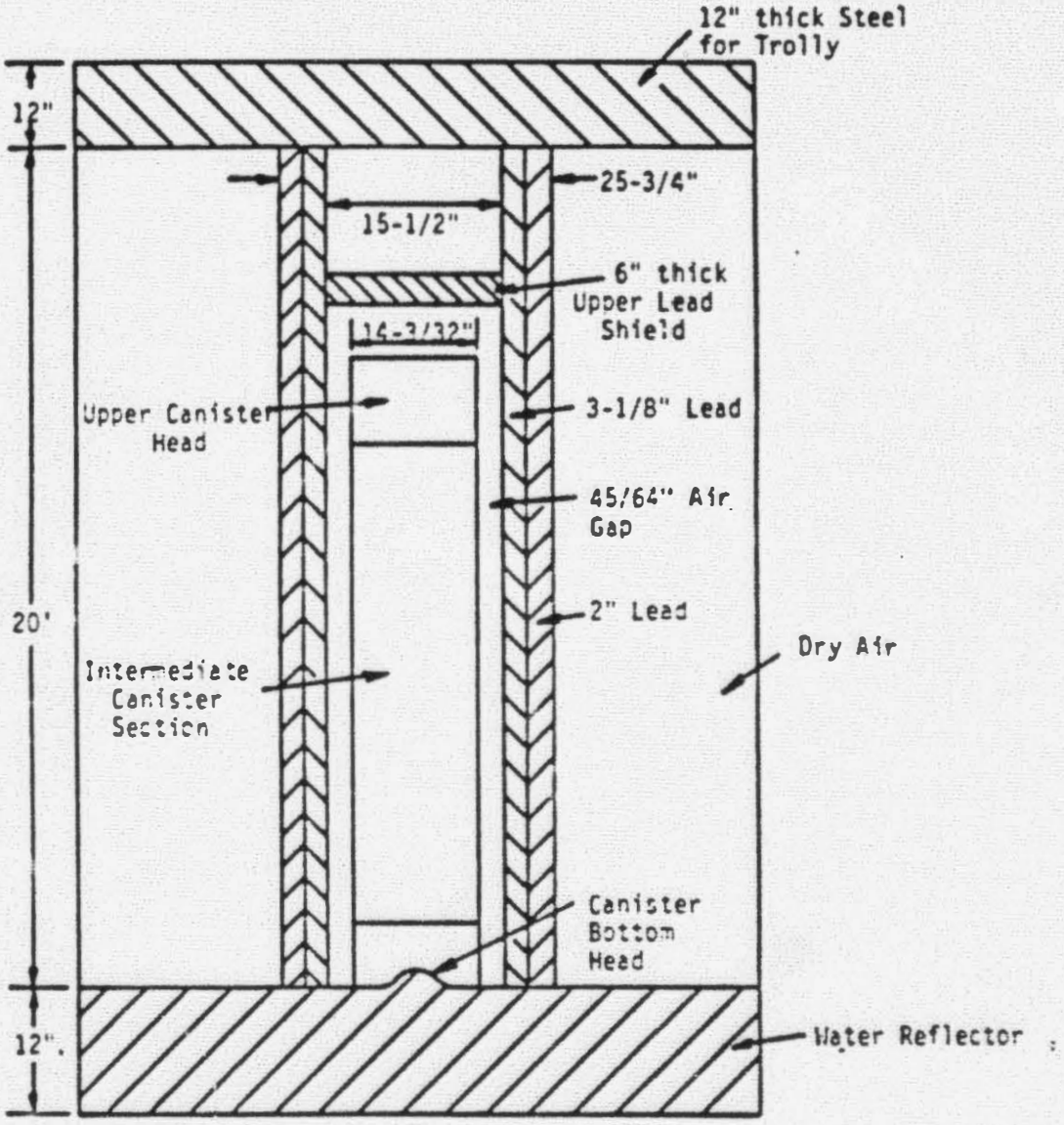

Figure 2

Revision 2 Transfer Shield Model

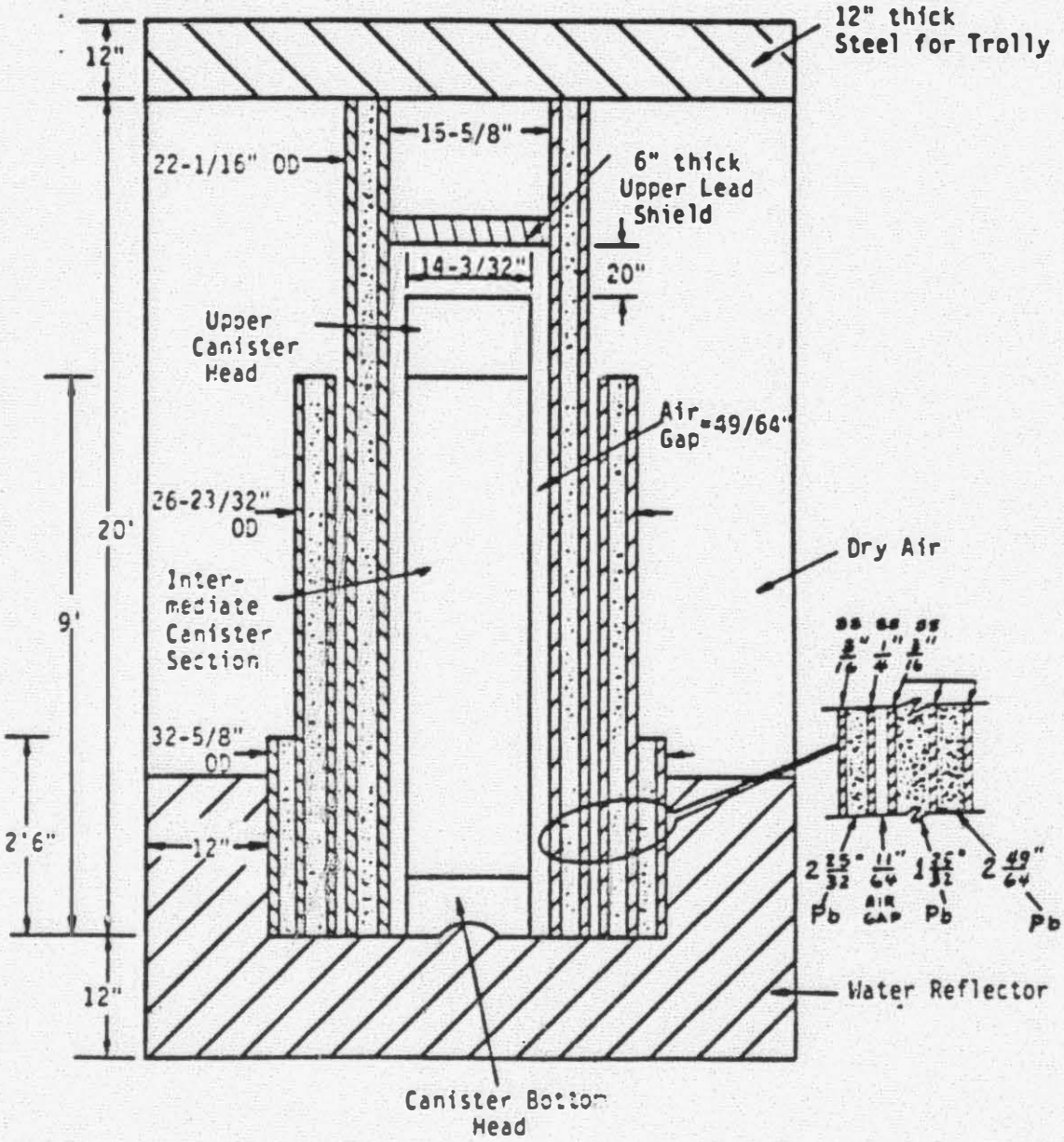

Figure 3

Transfer Shield Wall Cross-Section

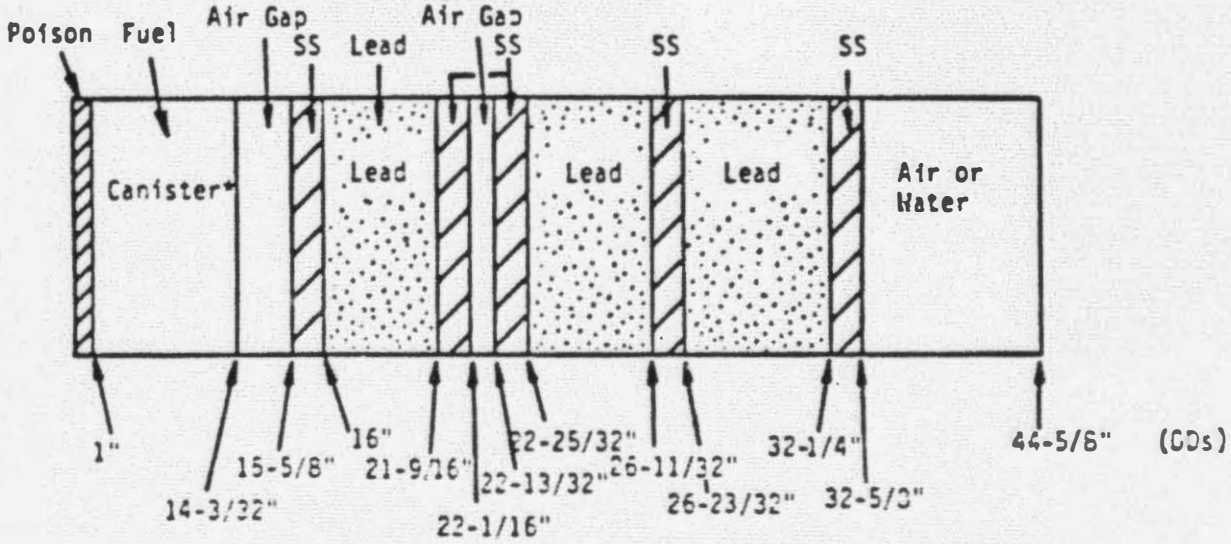

*All knockout canister detail not shown.

Figure 4

Transfer Cask Model

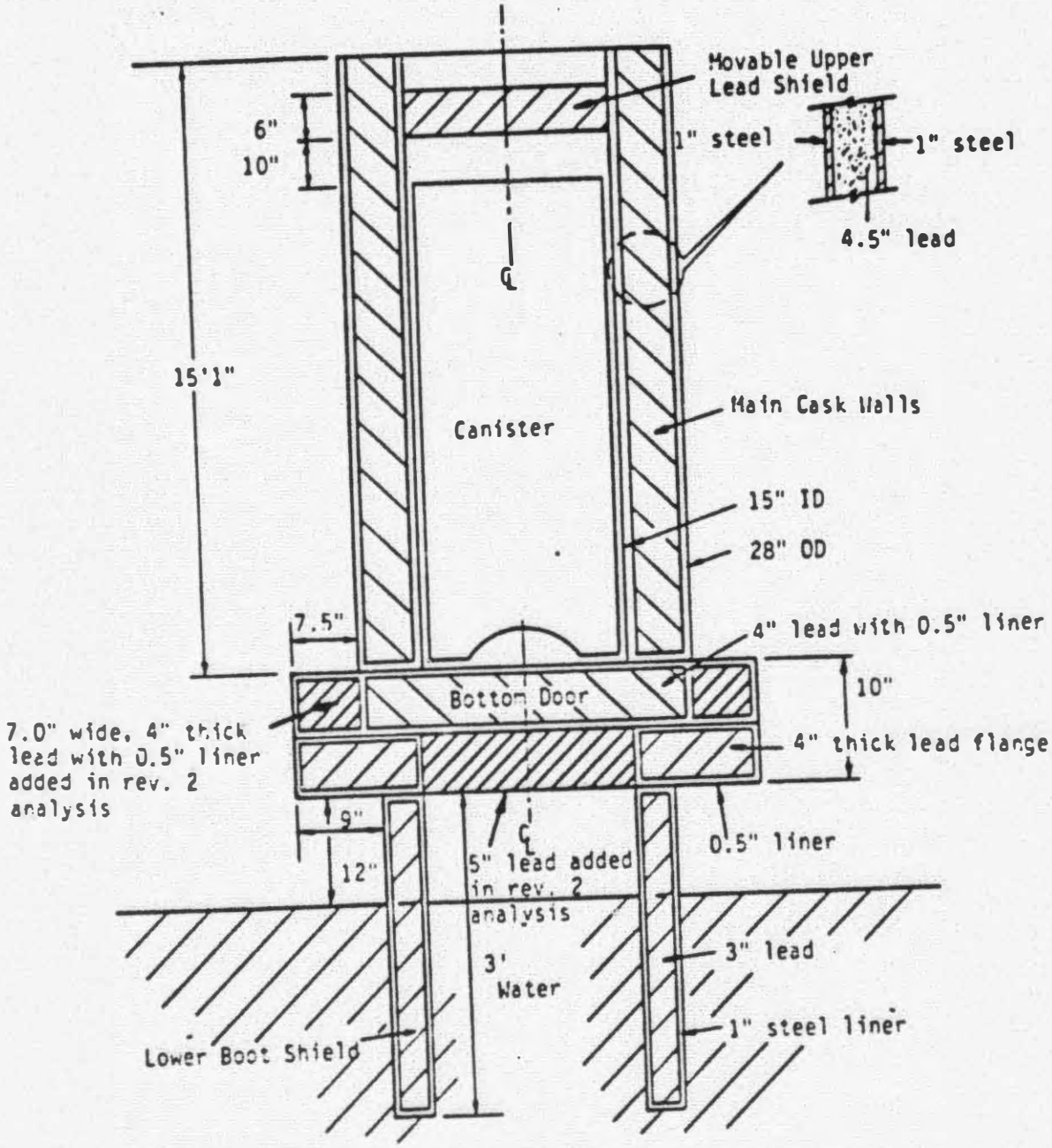

3.5 Dancoff Factor Assumptions

An obvious limitation in generating cross-sections for complicated geometrical configurations where differing fuel regions are involved is determining the effective Dancoff self-shielding effect on epithermal fuel resonances. The Dancoff factor using Sauer's method can be analytically determined for only the simplest geometries. In the case of the three canister designs, the fuel region geometries cannot be treated analytically with respect to Dancoff factors. In this analysis, it is only necessary to demonstrate that whatever Dancoff factors are utilized they result in the prediction of a conservative eigenvalue. For this purpose, the NULIF code was utilized. Evaluation of NULIF results with different Dancoff factors indicates that any increase in the Dancoff D=(1-C) factor from the infinite cell array condition results in a decrease in K-effective as a result of decrease U-238 self-shielding. Results also indicate that the potential decrease in K-effective is greater for higher density fuel. In the determination of Dancoff factors for cross-section sets used by KENOIV and XSDRNPM, infinite cell array conditions will be assumed for conservatism.

3.6 Computer Codes and Cross-Sections

The computer codes used in this work were NULIF[9], NITAWL[10], XSDRNPM[11], and KENOIV[12]. The NULIF code was used only for the study of Dancoff factor effects. NITAWL and XSDRNPM were used for processing cross-sections from the 123 group AMPX master cross-section library[13]. NITAWL provides the resonance treatment and formats the cross-sections for use by either XSDRNPM or KENOIV. In all cases, XSDRNPM cell weighted cross-sections are used by KENOIV and XSDRNPM/ANISN type calculations.

3.7 KENOIV Bias

No benchmark results are included in the current workscope to allow a direct assessment of the KENOIV bias for a fuel/lead system. However, the comparison of results between critical experiments and KENOIV[14,15] indicates a trend of increasing KENOIV bias related only to the spacing between fuel assemblies with no discernable trend due to materials placed between assemblies. The materials placed between the assemblies were stainless steel, aluminum, and B_4C rods, they provide a sufficient density change to indicate if there is a related bias. This assumption is carried over for the single canister, where it is assumed that the KENOIV bias is not dependent upon the reflector density. Thus, the bias for this case is assumed to be that of the single canister in water (i.e., 0.02 Δk)[3].

3.8 Fuel Optimization for Lead Shielded Canisters

3.8.1 Background Information and Assumptions

Of interest in this extension of the fuel optimization study is the effect of the external lead shield which makes up the transfer shield and transfer cask. To examine the effect of the lead shield on the optimized fuel mixture, simplified KENOIV and XSDRNPM models were utilized. Assumptions used in this optimization study which were based on previous canister studies contained in References 2 and 3.

3.8.2 Fuel Optimization Results

It was decided to benchmark KENOIV against XSDRNPM for simple cell types and to use XSDRNPM to quantify the effect of the lead shield. A simple 2D cell was run with KENOIV which consisted of a 14 inch diameter fuel region surrounded by water. No poison rods are modeled for these simple cases. This case was run .31 and .37 volume fraction cases and when taken with the infinite media NULIF results[2,3] predict the .31084 fuel volume fraction to be optimum. These results are shown in Table 1. Two XSDRNPM cases were run for a 13.5 inch diameter fuel region with a 1/4 inch thick steel outer shell surrounded by water. These XSDRNPM results also indicate the .31084 volume fraction is optimum and are shown in Table 1.

A six inch lead shield was modeled around the outside of the 14 inch canister in XSDRNPM. The lead shield had a 15.5 inch inside diameter resulting in a .75 inch dry air gap between the canister and the lead shield. Dry air was also modeled outside the six inch thick lead shield. Six inches of lead was chosen since it was considered to be the maximum thickness of the lead for either the transfer shield or transfer cask. No modeling of the steel liners on the shielding was considered. Dry air was also considered to consist of pure oxygen.

Three lead shielded XSDRNPM cases were performed for volume fractions of .25, .31084, and .37. The resulting eigenvalues are shown in Table 1 and demonstrates for the lead shield cases that the optimum fuel volume fraction remains as .31084. For the .31084 fuel volume fraction a six inch lead shield causes a .055 increase in delta k-effective over the water moderated case. This is the result of both decreased absorption in hydrogen and the canister shell as well as epithermal backscattering of neutrons from the lead to the canister.

One final case was performed with XSDRNPM to determine the effect of a decrease in the water density for the fuel water mixture in the canister surrounded by lead. New NITAWL-XSDRNPM cross-sections were generated for the .31084 fuel volume fraction with a 95% nominal water density. The result was a decrease in K-effective of .015Δk due to the decreased hydrogen density and neutron thermalization.

TABLE 1

COMPARISON OF KENOIV AND XSDRNPM RESULTS FOR SIMPLE CELL TYPES WITH AND WITHOUT LEAD AND NO POISON RODS*

Cell Type	Model	Vol. Fraction	K-effective/2σ dev.	Neutron Histories	
14 inch dia. fuel, no steel, w/H_2O	KENOIV	.31084	1.07±.010	18963	(1)
14 inch dia. fuel, no steel, w/H_2O	KENOIV	.37	1.065±.008	19565	(1)
13.5 inch dia. fuel, 1/4 inch steel can, w/H_2O	XSDRNPM	.31084	1.0300	-----	(1)
13.5 inch dia. fuel, 1/4 inch steel can, w/H_2O	XSDRNPM	.37	1.0195	-----	(1)
13.5 inch dia. fuel, 1/4 inch steel can, w/air gap and 6 inch lead shell	XSDRNPM	.25	1.0797	-----	(1)
13.5 inch dia. fuel, 1/4 inch steel can, w/air gap and 6 inch lead shell	XSDRNPM	.31084	1.0853	-----	(1)
13.5 inch dia. fuel, 1/4 inch steel can, w/air gap and 6 inch lead shell	XSDRNPM	.37	1.0712	-----	(1)
95% Nominal H_2O Density	XSDRNPM	.31084/ 95% H_2O	1.0703	-----	(1)

*The absolute magnitude of K-effective is not significant. Simple cell results are only used to indicate trends.

3.9 Canister-Shield Gap Criticality Analysis

3.9.1 Model Description and Background

When the transfer shield is lowered into the pool to allow inserting of a canister, part of the gap region between the transfer shield and canister will be water filled and part of it may contain only air. To determine the most critical canister configuration in the shield, it is necessary to quantify the effect of the .75 inch gap region. For this analysis, XSDRNPM was used since the changes in reactivity due to the gap are small and would not be suited for a Monte-Carlo code with its associated uncertainties. Two additional XSDRNPM cases were run for the optimal fuel volume fraction of .31084 with 50°F nominal density water and 5% dense water in the gap region. The lead shield was assumed to be six inches thick and the canister was modeled as a 13.5 inch diameter fuel region with a 1/4 inch steel shell. No poison rods are modeled in these simple canister types.

3.9.2 Gap Analysis Results

The results shown in Table 2, which include two cases from the fuel optimization study, demonstrate that the most reactive configuration occurs whith an air gap between the lead shield and canister. These results are explained by the backscatter of neutrons from the lead shield to the water filled canister. The air between the canister and shield attenuates fuel neutrons and does not contribute significantly to the thermal neutron spectrum. Without the consideration of 3D geometry induced leakage effects, these results predict the most critical configuration for a canister is to be fully inserted into the transfer shield.

TABLE 2

XSDRNPM K-EFFECTIVE RESULTS FOR CANISTER-SHIELD GAP ANALYSIS*

Model Description	K-effective	
Fuel Canister (14 inch dia.) and water only	1.030	(1)
Fuel Canister (13.5 inch dia. fuel, 1/4 inch steel shell, .75 inch water gap, 6 inches lead)	1.066	(1)
Fuel Canister (13.5 inch dia. fuel, 1/4 inch steel shell, .75 inch 5% water density gap, 6 inches lead)	1.0848	(1)
Fuel Canister (13.5 inch dia. fuel, 1/4 inch steel shell, .75 inch air gap, 6 inches lead)	1.0853	(1)

*The absolute magnitude K-effective is not significant. Simple cell results are only used to indicate trends.

3.10 Transfer Shield Water Reflector Analysis

3.10.1 Model Description and Background

Revision 1 analysis did not have water modeled on the outside of the transfer shield because when the canister is fully inserted into the shield it is above the water level. This was determined to be the most reactive insertion point (see Section 3.13, Canister Insertion Analysis). Additionally, the XSDRNPM gap analysis (Section 3.9) demonstrated that an air or void filled gap is most reactive. In the subsequent Revision 2 analyses that incorporate the latest knockout canister geometry, is was theorized that a 2 ft. high water reflector outside the shield may help reflect neutrons back to canister and prove to be an additional conservative modeling assumption. Therefore, in Revision 2 transfer shield analyses, the following conservatisms will be implemented.

1. The outer movable shield will be completely raised to maximize the total lead and steel thickness,

2. The water level of the pool will be raised to a height 2 ft. from the bottom of the transfer shield to help reduce leakage,

3. The canister-shield gap region will be assumed to consist entirely of air to maximize reactivity of the system, and

4. Water will be assumed along the bottom of the canister to reduce leakage and prevent neutron streaming (compare Figures 1 and 2).

3.10.2 Water Reflector Results

Two cylindrical XSDRNPM cases were performed modeling a canister with a central poison rod surrounded by the transfer shield geometry according to Figure 3. One case was run with a 1 ft. wide air reflector and one with a 1 ft. water reflector. In both cases the canister shield gap region was filled with air to be consistent with the conservative manner in which later 3D KENOIV transfer shield cases would be run. The results of this analysis, shown in Table 3 demonstrate that the water reflector external to the lead shield is a positive reactive addition by reducing neutron leakage. The difference in K-effective for these two cases is approximately .0081Δk. The 2 ft. increase in water level above the canister bottom in the external region around the shield comprises only 16.4% of the knockout canister length. Since the XSDRNPM calculation is modeling the water region over the entire length of the shield the reactivity increase in the 3D KENOIV model is much less than .0081Δk. It is also important to recognize that the bottom canister region has less neutron importance than the middle regions of the canister. For simplicity, if we assume all canister regions are equally important, it is expected that the increase i K-effective of this already conservative model would be approximately .0013Δk.

For the early Revision 1 analysis, this increase in K-effective from the 2 ft. water level is more than offset by the extension of the outer lead shield the full length of transfer device. Additionally, if the entire canister shield gap region contained water instead of air, K-effective based on XSDRNPM results would drop by approximately .0193Δk (see Section 3.9). Therefore, the gap region between the canister and shield appears to be worth more in terms of reactivity than the water or air region surrounding the lead transfer shield. For these reasons the calculated K-effectives from the Revision 1 transfer system analysis are conservative. Although it is recognized that is is physically impossible to have an air gap between the canister and shield and have water outside the shield at the same level, this charge was implemented in all Revision 2 transfer shield analyses.

TABLE 3

XSDRNPM WATER REFLECTOR ANALYSIS*

Model Description	K-effective	
Canister in steel and lead shield, air gap, and air reflector	1.02742	(2)
Canister in steel and lead shield, air gap, and water reflector	1.03548	(2)

*The absolute magnitude K-effective is not significant. Simple cell results are only used to indicate trends.

3.11 Off-Centered Canister in Transfer Shield

3.11.1 Model Description and Background

To assess the effect of a canister that is off-center in the transfer shield or swinging from side-to-side within the shield, the XSDRNPM code was utilized. The off-centered canister was modeled inside the shield using 1D slab geometry with a buckling factor to allow axial leakage. The entire diameter of the shield was modeled plus 1 ft. of air on either side. The gap region was assumed to contain air. Shown in Figure 5 is the geometry detail of the off-centered canister case. The thickest lead region of the transfer shield was modeled since this would maximize the number of reflected neutrons to the canisters. The two inch poison rod in the center of the canister was also modeled.

3.11.2

The results for centered and off-centered canister XSDRNPM calculations are shown in Table 4. For the centered canister case the gap modeled is 49/64 inches on either side of the canister. For the off-centered case, the total gap width 1-17/32 inches is modeled entirely on one side of the canister with the outer side flush against the steel-lined lead wall. Examination of the results of these two cases indicate that the difference in K-effective is approximately .0001Δk which is considered negligible. Additionally, the centered canister is most reactive. Therefore, for the remainder of this analysis all canisters will be assumed to be centered within the respective shields.

Figure 5

Off-Centered Canister XSDRNPM Model

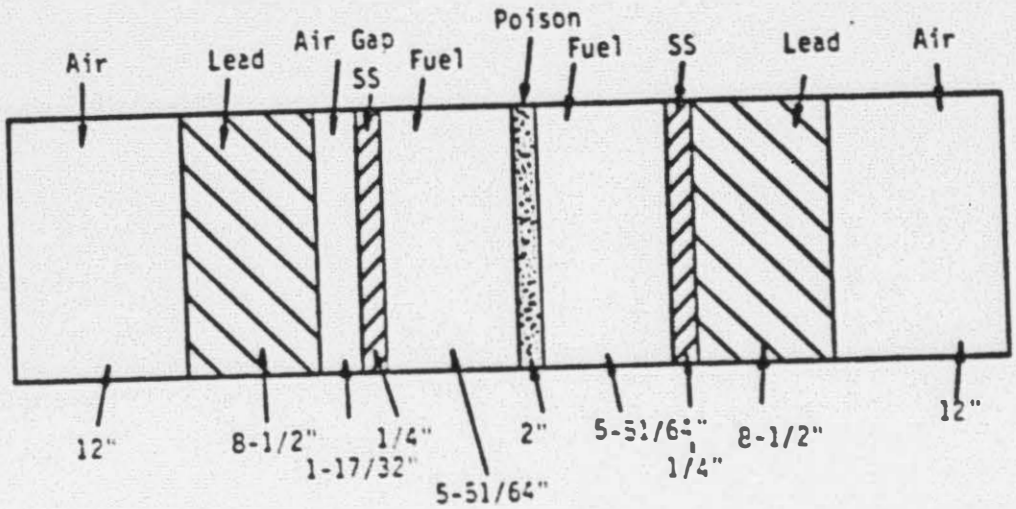

TABLE 4

XSDRNPM K-EFFECTIVE RESULTS FOR OFF-CENTERED CANISTER*

Model Description	K-effective
Centered Fuel Canister	1.05547
Off-Centered Fuel Canister	1.05534

*The absolute magnitude K-effective is not significant. Simple cell results are only used to indicate trends.

3.12 Canister Optimization in Transfer Shield

3.12.1 Model Description and Background

For determining which canister type is most reactive in the transfer shield and the similar transfer cask, a 3D KENOIV transfer shield model was used. For conservatism in Revision 1 analyses that 9 ft. long outer shield was extended the full length of the transfer shield. In a similar manner the 16 ft. long inner shield was extended to the water level. The steel inner and outer liners on each shield and the air gap were modeled as lead giving a combined thickness of 5.125 inches. A circular shaped 3 inch lead plate is located 20 inches above the top of the canister. A smaller 3 inch lead shield is located within the canister grapple. These two shields were combined to form one 6 inch lead shield 20 inches above the canister. Although few neutrons will penetrate the 6 inch circular shield, the rest of the transfer shield was modeled by an additional 7.84 ft. of shielding with a 1 ft. thick block of steel placed horizontally on top of the shield to represent the trolly underframe. The total length of the thickened lead shield and trolly underframe is 21 ft. This structure is surrounded by 1 ft. of water (up to the bottom of the shield) on all sides. The transfer shield was not extended below the water surface in the original analyses since it was shown by previous XSDRNPM calculations in Table 2 that the lead shield with an air gap is most reactive. The water level was also extended to the bottom of the canister and shield to preclude neutron streaming out of the transfer shield when the outer shield is raised. The previously described transfer shield model is shown in Figure 1.

The ruptured knockout and filter canisters were modeled in 3D with this transfer shield model to determine which canister type is most reactive. The fuel assembly canister was not considered since concrete will be placed in the outer lobes an will prevent the more reactive ruptured configuration. For canisters with this concrete modification in a 17.3 inch array, K-effective is 0.829 ± 0.025[3]. This K-effective is low enough relative to the knockout canister 17.3 inch lattice K-effective[3] that the fuel canister can be eliminated from consideration.

3.12.2 Transfer Shield Optimization Results

The results of the transfer shield analysis with the ruptured knockout and filter canister fully inserted into the shield demonstrate the knockout canister to be most reactive. These results are shown in Table 5 and indicate that the ruptured knockout canister is $0.36 \pm 0.14 \Delta k$ more reactive than the ruptured filter canister in the transfer shield. The respective increase in K-effective from the lead shield for the knockout and filter canister cases is $0.43 \pm .018$ and $.045 \pm 0.18$. It should be recognized that the no shield cases in Table 5 were taken from Reference 2, and have an overly high K-effective from the previously documented U-238

cross-section treatment. If the 0.15Δk conservatism[3] is subtracted from these results, the increase in K-effective from the 5.125 inch lead shield becomes .058±.018 and .060±.018, respectively. for the two cases examined. This increase in reactivity is in good agreement with the .055Δk reactivity increase from XSDRNPM results discussed in the optimization analysis. Based on the results of Table 5, the ruptured knockout canister was used in subsequent analysis of the transfer shield and cask.

TABLE 5

CANISTER - TRANSFER SHIELD OPTIMIZATION RESULTS

	K-effective/2σ	Keno Bias	Max. K-effective	Histories	
Transfer Shield** w/Knockout Canister	.887±.009	.02	.916	21371	(1)
Transfer Shield** w/Filter Canister	.851±.011	.02	.882	18361	(1)
Single Knockout* Canister, No Shield	.844±.016	.02	.880	10234	(1)
Single Filter* Canister, No Shield	.806±.014	.02	.840	9331	(1)

*From Reference 2.
**These cases were run for a canister shield gap of 0.5 inches.

3.13 Canister Insertion Analysis

3.13.1 Model Description and Background

From the canister optimization study, it was determined that the knockout canister was the most reactive canister type. For that analysis it was assumed, based on XSDRNPM results, that a canister fully inserted into the transfer shield was the most reactive configuration. This assumption is verified by the insertion study described in this section.

The basic transfer shield model is the same as that described in the canister optimization study. To simplify the generalized geometry, the canister will be raised into the shield with the water level flush with the bottom of the shield to prevent neutron streaming. The outer shield will not be extended below the water surface since XSDRNPM results from the gap study indicated that lead with an air gap is more reactive than lead with a water gap approximately 1.9%$\Delta\sigma$. The horizontal six inch lead shield will be maintained 20 inches above the canister upper head even though the downward travel of this shield is limited to the lower end of the inner shield. This approximation is conservative for the smaller percentage insertion cases because the 6 inch horizontal shield will be modeled closer to the upper head than it should be maximizing K-effective.

Figure 6 shows the knockout canister at its 6.8, 54.4, 96.6, and 100% insertion levels. These levels correspond to the different geometry block boundaries. Other insertion levels were used to generate the insertion curve shown in Figure 7. Although the problem "snapshot" changes in Figure 6 as the knockout canister is inserted into the shield, the area being modeled is sufficiently large that material effects external to the problem boundary are insignificant in the computation of K-effective. This is true in the water moderated region where a minimum of 12 inches of water is used, effectively decoupling the canister from other pool materials. Neutrons that do penetrate the lead shield above the water surface stream through the air medium and would probably not return to the canister-shield system. Effects of the pool walls and other concrete structures were not considered since pool-wall reflector calculations in Referenced 2 and 3 demonstrate that concrete behaves in a fashion similar to water. The effect of the concrete will be to thermalize most neutrons escaping from the lead shield, they would be subject to absorption in the steel canister shell and gap medium prior to reaching the fuel water mixture. Finally, the water reflector analysis of Section 3.10 demonstrated that if the entire transfer device were surrounded by water, the most K-effective could increase from reduced leakage is .0081 Δk. Since it is not possible to completely surround the shield with concrete, any increase in K-effective from walls or other structure will be small. For these reasons, it is felt that an external concrete structure near the transfer shield or cask will have a negligible impact on the calculated K-effective.

3.13.2 Canister Insertion Analysis Results

The results of the Transfer shield insertion study with the knockout canister are tabulated in Table 6 and shown in Figure 7. These results confirm the XSDRNPM results that the most reactive configuration is for the knockout canister fully inserted. The cases performed for the Revision 1 insertion study used the knockout canister model that does not reflect the recent 3.75 inch reduction in the four outer B_4C poison rods. The 3.75 inch reduction in length represents only a 2.8% reduction in the total poison length and should not result in a more significantly limiting insertion case.

Figure 6

Typical Ruptured Knockout Canister Insertion Levels in Transfer Shield

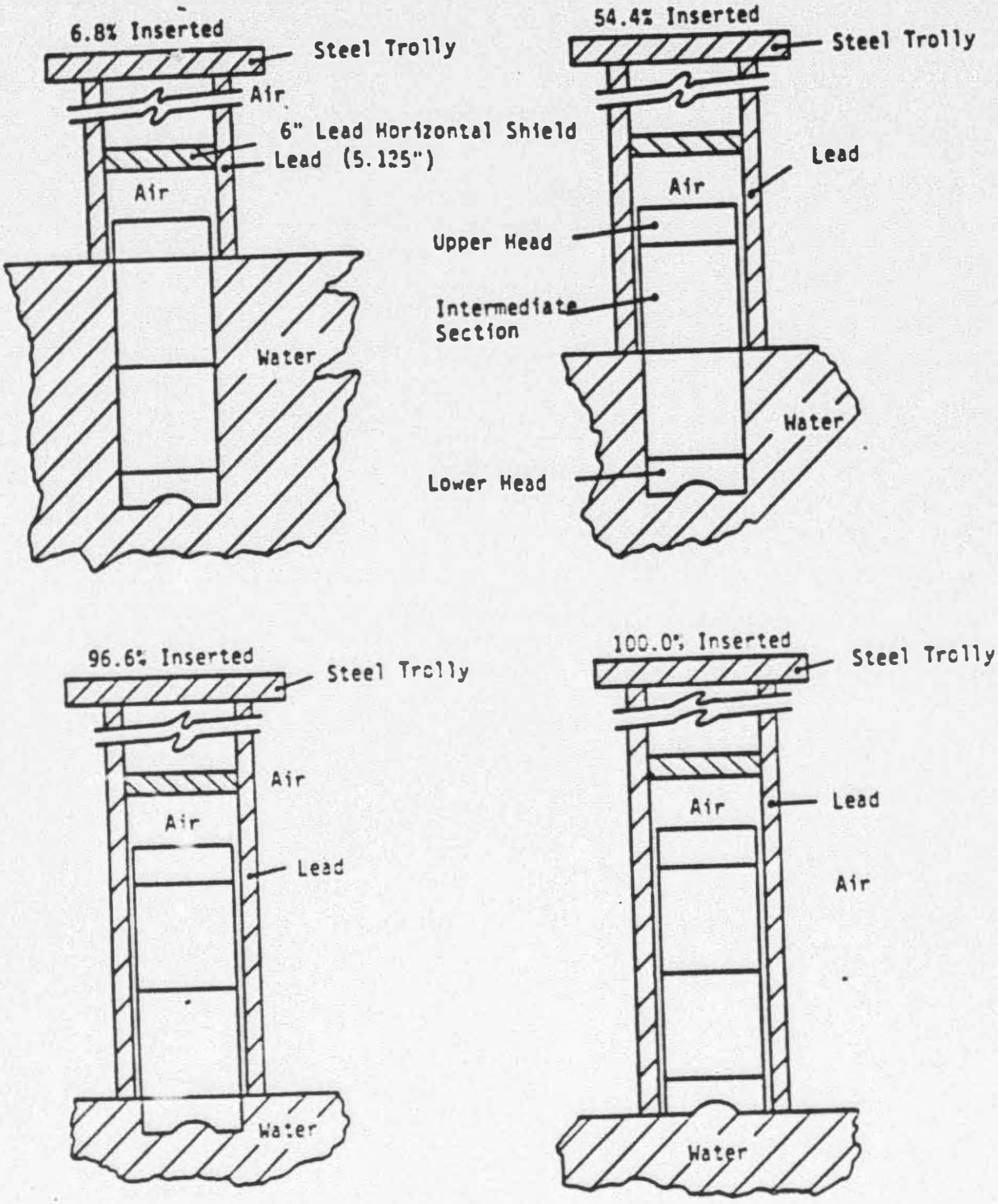

This effect was verified by computing the ruptured knockout canister case fully inserted into the transfer shield with the shortened rods. The resultant K-effective was .002 smaller than the case with longer rods and is shown in Table 6. This difference in K-effective is insignificant since it is smaller than the .006-.007 2σ KENOIV uncertainty. Because of the insignificance of the B_4C rod length change on K-effective values, the original studies are valid for the current design. Since the transfer cask is similar to the transfer shield, the fully inserted position should be optimum for the cask, especially with the cask lead door closed.

Also included in Table 6 is a reanalysis of the ruptured knockout canister 100% inserted into the transfer shield. The transfer shield was modeled according to dimensions in Figure 2. Differences between this calculation and earlier analysis are:

1. The exact height of the outer 9 ft. and 30 inch shields are modeled.

2. The water reflector outside of the shield is raised 2 ft.

3. The new knockout canister geometry with baffle plate modifications and poison rod length reductions are implemented.

4. The steel liners are modeled in the shield walls.

With the above modifications, the resultant K-effective is 0.879±.01 which yields a maximum K-effective with the KENOIV bias of .909. The results are consistent with the Revision 1 analysis indicating the earlier cases are sufficiently conservative.

Two additional cases were calculated for the transfer shield. The first case utilized the NULIF code to determine an optimum fuel-water volume fraction with low density water. An optimum fuel volume fraction of 0.021 was determined for 0.05 g/cc dense water. This case was performed because of a concern that for low density water cases there could exist the possibility of secondary reactivity spike for an array of assemblies or canisters. Since lead and steel are good reflectors of neutrons this case was performed to ensure that neither the transfer shield or cask could imitate this array effect. As Table 6 indicates, K-effective is nearly zero due to the low fission density of neutrons. This low fission density is the result of the small optimized fuel volume at low water densities together with significant amounts of structural and poison material. The second case also utilized 0.05 g/cc dense water but for a fuel-water volume fraction of .31084. As shown in Table 6, this case yields a maximum K-effective of only .205. Therefore, it appears that the reactivity spike at low water densities does not occur for single canisters in lead shielded device.

TABLE 6

KNOCKOUT CANISTER INSERTION STUDY K-EFFECTIVE RESULTS

% Inserted	K-effective/2σ	KENO Bias	Max. K-effective	Neutron Histories	
100.0%	.882±.006	.02	.908	38354	(1)
86.0%	.881±.007	.02	.908	39864	(1)
65.0%	.875±.007	.02	.902	37448	(1)
54.4%	.866±.008	.02	.894	30200	(1)
42.4%	.855±.009	.02	.884	21744	(1)
22.8%	.836±.011	.02	.867	16610	(1)
6.8%	.827±.011	.02	.858	19328	(1)
100.0% (short rods)	.880±.007	.02	.907	42582	(1)
100.0% (new canister and shield geometry)	.879±.010	.02	.909	23655	(2)
Optimized Fuel (.021 VF fuel, 0.05 g/cc dense water)	.020±.001	.02	.041	16185	(2)
Low Water Density (.31804 VF fuel, 0.05 g/cc dense water)	.181±.004	.02	.205	16600	(2)

Examination of the scattering cross-section for iron in the epithermal range indicates that steel in air could be potentially as good of a reflector of epithermal neutrons as lead due to both cross-section magnitude and the higher number density of iron atoms. To investigate the significance of steel versus lead in an air medium, three XSDRNPM cases were performed with cylindrical geometry. The cases performed consisted of a shield containing a thickness of 8.5 inches of lead, one containing 8.5 inches of steel, and one with 8.5 inches of alternating layers of steel and lead according to Figure 3.

Figure 7

Reactivity Dependence of Knockout Canister Insertion Into Transfer Shield

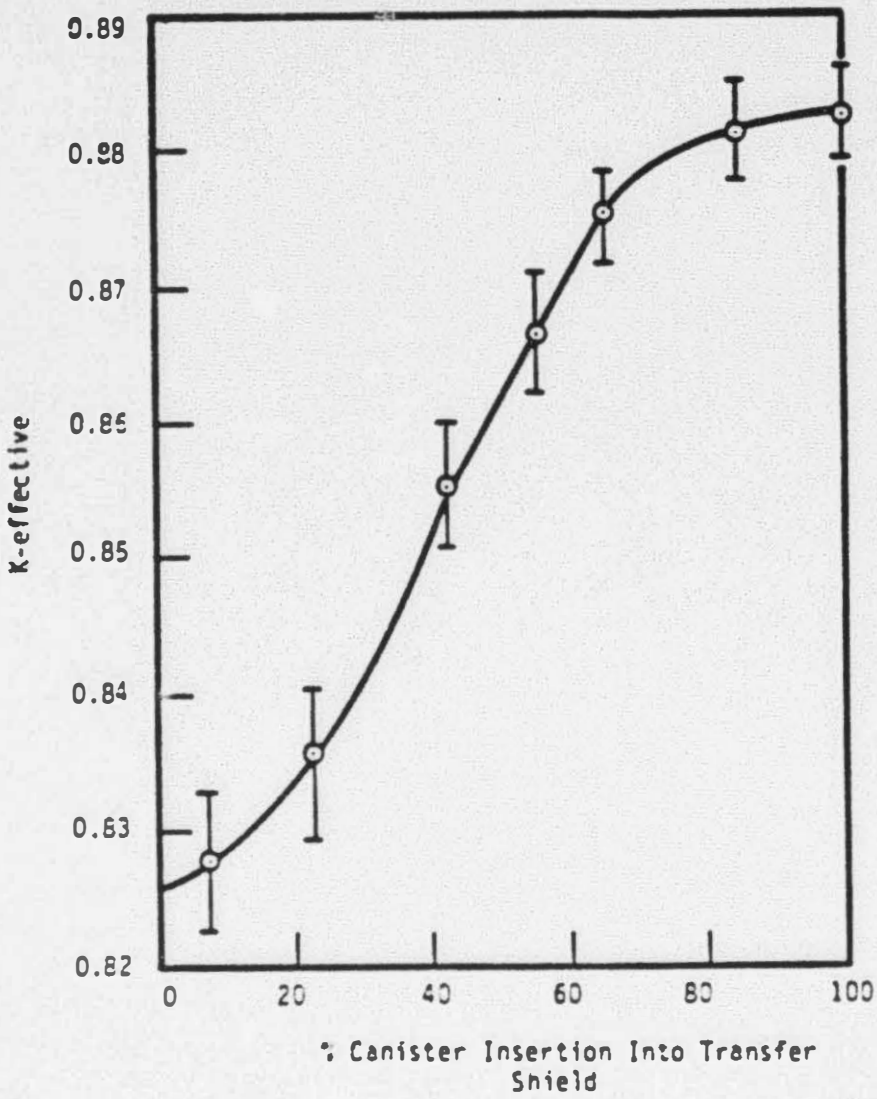

For the XSDRNPM results shown in Table 7, the all steel shield is more reactive than the all lead shield case by .004 Δk.

However, when steel and lead are combined, there is a decrease in K-effective relative to the all lead case of 0.002 Δk. This decrease in K-effective is currently thought to be a space-energy interaction between the steel and lead. Since both the transfer shield and cask have alternating layers of steel and lead, the steel liners in all Revision 2 analyses are modeled.

TABLE 7

XSDRNPM STEEL LINER ANALYSIS*

Cell Type	Model	K-Effective	
14 inch canister, air gap, 8.5" steel shield	XSDRNPM	1.03371	(2)
14 inch canister, air gap, 8.5" lead shield	XSDRNPM	1.02961	(2)
14 inch canister, air gap, 8.5" shield with alternating layers of steel and lead	XSDRNPM	1.02742	(2)

*The absolute magnitude of K-effective is not significant. Cell results used to indicate trends.

3.14 Transfer Cask Analysis

3.14.1 Model Description and Background

The transfer cask is shown in Figure 4. The 15 ft. 1 inch long upper lead shield is 4.5 inches thick with an additional 1 inch steel liner in both sides. A 6 inch thick horizontal lead shield, located 10 inches above the upper head of the knockout can is assumed. The bottom lead door, shown in the closed position in Figure 4, is 4 inches thick with an additional 0.5 inch of steel liner on all sides. For Revision 2 analysis only, the region below the 4 inch lead door was filled with lead to add an extra 5 inches of lead for conservatism. This given a combined lead and steel thickness below the canister of 10 inches. It is assumed the door consists of two hemi-cylinders that can be opened. For conservatism in Revision 2 calculations only, the door was extended to an outside diameter of 43 inches and is indicated in Figure 4. Located below the bottom door is a lead shield flange that projects 7.5 inches in a radial direction beyond the main cask walls. This lead flange is also 4 inches thick with an additional 0.5 inch thick steel liner on all sides. The total length of the flange is 14 inches. A lower shield collar, called a loading boot was included in the model and extends 2 ft. into the pool. The loading bot has a 3 inch lead thickness with a 1 inch steel liner on all sides. The total length of this collar is assumed to be 3 ft. Although the loading boot is no longer required, it was maintained for conservatism since the inside diameter of the loading boot is less than the optional vertical shield used with the cask. The inside diameter of the transfer cask is assumed to be 15 inches resulting in a 0.5 inch air gap between the canister and the inner cask wall steel liner.

3.14.2 Cask Analysis Results

Since it was determined from the transfer shield insertion study that the fully inserted canister in most reactive, calculations during the ruptured knockout canister were performed with the canister fully inserted and the bottom lead door closed. Results from the ruptured knockout canister fully inserted into the transfer cask are shown in Table 8. These results indicate that with the 2σ uncertainty and KENOIV bias added, the maximum K-effective is less than the .95 criteria. This calculation was performed for the ruptured knockout canister with the original longer B_4C rods. The previous insertion study demonstrated that the reduction in poison length by 3.75 inches resulted in a effect on K-effective of less than the 2σ uncertainty of the calculation.

It was not expected that the external lead/steel flange would have any significant impact on the worst reactive insertion position since this flange is 10 inches thick and would cover only a 2.8% slice of the canister at any time during insertion. To verify this assumption and to simplify geometry

modifications, early calculations were performed with an additional 10 inch thick lead/steel collar, 7.5 inches thick radially, that was added to the outside of the cask at the approximate midplane of the knockout canister. This position will be nearly the most reactive position for this canister design. Additionally, the outer B_4C rods were 3.75 inches shorter. This case in all other respects is the same as the previous case with longer rods. Since both the additional lead and shorter B_4C rods are positive reactivity additions, the close reactivity agreement between the first and second cases indicates that the change in poison rod length and additional lead collar have an insignificant effect on reactivity. These calculations are in close agreement with the transfer shield insertion study which also indicated the difference in B_4C length to be within the KENOIV uncertainty.

One additional cask case was run which utilized the exact geometry of the knockout canister with the revised baffle plate positions and poison rod lengths. In addition, extra lead was added below the bottom door and in the flange region for conservatism. This case shown in Table 8 is the most limiting of all cases examined with a maximum K-effective of .931.

The results of the insertion analysis for the ruptured knockout canister in the transfer cask indicate that criticality criteria will not be violated. It is, therefore, reasonable to assume that no borated polyethylene liner will be required as a reactivity control device for either the transfer shield or cask. No analysis has been made of externally damaged or deformed canisters since these canisters will be handled by GPU Nuclear on a case by case basis and, therefore, are not included in the current workscope.

TABLE 8

K-EFFECTIVE FOR THE RUPTURED KNOCKOUT CANISTER IN THE TRANSFER CASK

% Inserted	K-effective/2σ	KENO Bias	Max. K-effective	Neutron Histories	
100% (Longer B_4C rods)	.897±.006	.02	.923	47725	(1)
100% (Shorter B_4C rods and extra lead collar)	.897±.007	.02	.924	43990	(1)
100% (Latest geometry and extra lead)	.904±.007	.02	.931	40255	(1)

4.0 CONCLUSIONS

With the canister design assumptions defined by References 2 and 3 and unique cross-section sets generated by the NITAWL-XSDRNPM codes, the optimal fuel volume mixture was demonstrated to remain as .31084 with a 6 inch lead shield. Conditions of water at 50°F and 100% nominal density were demonstrated to be most reactive.

The most reactive compositions for the gap region between the canister and transfer cask or shield lead wall was shown to be either void or air. Partial mixtures of water and air pure water were shown to be less reactive compositions for the gap region. Water regions surrounding the lead shield were shown to be small positive reactivity additions and less than the gap effect. XSDRNPM slab calculations demonstrated that there was almost no change in K-effective for an off-centered canister within the transfer shield with the centered position being most reactive.

Insertion studies with the transfer shield demonstrate that the knockout canister is the most reactive of the three canister designs. The presence of a transfer shield provides a reactivity increase over the single canister in water of approximately (.055 to .06Δk) ± .018Δk. The insertion analysis also defined the 100% insertion level as the most reactive configuration for a canister either the transfer shield or cask. Modeling the steel liners within the transfer shield wall as well as other modeling changes resulted in K-effective being nearly the same as that computed by earlier shield models. Therefore, previous analyses for the transfer shield are sufficiently conservative. XSDRNPM calculations verified that an all steel liner is more reactive than an all lead liner by 0.004ΔK. A combined steel and lead liner was found to be 0.002Δk less reactive than the all lead shield. Further analyses for the transfer shield with a reduced water density of 0.05 g/cc verified that there is no secondary reactivity spike for low water density cases. Analyses were performed for the knockout canister in the transfer shield and cask with the 3.75 inch shortened outer B_4C rod modification. These results demonstrated that the reactivity increase due to the slightly shorter outer B_4C rods is less than the KENOIV uncertainty. The effect of the lead/steel flange was conservatively quantified by placing an additional lead collar around the middle of the transfer cask at potentially the most reactive position with a knockout canister fully inserted. Since the collar could cover only 2.8% of the canister at any time during insertion, the reactivity effect was shown to be less than the KENOIV uncertainty and calculationally insignificant. A cask case was performed implementing the latest knockout canister geometry which exactly models the shorter poison rods and the revised baffle plate locations. Extra lead was added to the bottom door and flange region of the cask for conservatism. This case was the most limiting with a maximum K-effective of 0.931.

Results of these analyses indicate that no borated polyethylene or other poison material is required in the design of the transfer shield or cask for reactivity control. These results are valid for standard unruptured canisters and canisters with internally ruptured filter screens containing fuel in upper and lower head regions. Canisters with extensive internal damage and/or external damage from being dropped and deformed are not addressed since these canisters will be handled by GPU Nuclear on a case by case basis and, therefore, are not included in the current workscope.

5.0 REFERENCES

1. "Canister Transfer System Information," 38-1013198-00, December 4, 1984

2. "TMI-2 Defueling Canisters Final Design Technical Report," Document 77-1153937-00 (B&W), October 31, 1984

3. "TMI-2 Defueling Canisters Final Design Technical Report," Document 77-1153937-04 (B&W), May 1985

4. "Technical Specification for Design of Defueling Canister for GPU Nuclear Corporation Three Mile Island - Unit 2 Nuclear Power Plant," 53-1021122-01 (B&W), Revision 2, July 17, 1984

5. "Licensing Requirements for the Storage of Spent Fuel in an Independent Spent Fuel Storage Installation," 10 CFR 72, U.S. Nuclear Regulatory Commission, Revision 1, May 1977.

6. "Nuclear Criticality Safety in Operations with Fissionable Materials Outside Reactors," American National Standards Institute, American National Standard, ANSI/ANS 81, 1983

7. "Criticality Safety Criteria for the Handling, Storage, and Transportation of LWR Fuel Outside Reactors," American National Standards Institute/American National Standard, ANSI/ANS 8.17, 1984

8. "Guide for Criticality Safety in Storage of Fissionable Materials," American National Standard, ANS 8 7/N16.5, 1982

9. "NULIF - Neutron Spectrum Generator, Few Group Constant Calculator and Fuel Depletion Code," BAW-426, Revision 5, January 1983

10. "NITAWL Nordheim Intergral Treatment and Working Library Production," (B&W Version of ORNL Code - NITAWL), NPGD-TM-505, Revision 5, June 1984

11. "XSDRNPM AMPX Module with One-Dimensional Sn Capability for Spatial Weighting," AMPX-II, RSIC-RSP-63, ORNL

12. "KENO4, An Improved Monte Carlo Criticality Program," (B&W Version of ORNL Code, KENOIV), NPGD-TM-503, Revision B, August 1982

13. W.R Cable, "123 Group Neutron Cross Section Data Generated From ENDF/B-II Data for Use in the XSDRN Discrete Ordinates Spectral Arraying Code," RSIC-DLC-15, ORNL, 1971

14. M.N. Baldwin, et.al., "Critical Experiments Supporting Close Proximity Water Storage of Power Reactor Fuel," BAW-1484-7, July 1979, (B&W) (available from National Technical Information Services), Revision 0

15. F.M. Alcorn, Nuclear Criticality Safety Benchmark Notebook," Revision 2, February 1984 (LRC Document)

ATTACHMENT 2

ASSESSMENT OF A DRAINED POOL SCENARIO

The results of this analysis are based on the assumption that the most reactive fuel particle capable of being in the knockout canister is an optimally moderated, standard, whole fuel pellet. With the change to the vacuum system that permits fuel particles greater in size than whole pellets to be loaded into a knockout canister this assumption is no longer appropriate. The analysis in this statement has been completed using conservative assumptions (e.g., neglected four satellite poison tubes). Additionally, the probability of a drained pool scenario occurring is small. Therefore, the analysis was not repeated using optimum size fuel particles, however, the conclusion that k_{eff} will not exceed 0.99 for a drained pool scenario is still considered appropriate.

TMI-2 DRAINED POOL ANALYSIS

Cases Analyzed

Two drained pool cases representing different states of internal transfer moderation are considered here. These cases are judged to be bounding with respect to the possible real contents of the canisters in the unlikely event of loss of pool water. The conditions assumed for these cases are as follows:

Case 1: Optimal fuel volume fraction in 4350 ppm boron moderator of full density at 50°F.

Case 2: Realistic fuel volume fraction with pure water moderation at 100% humidity conditions at 50°F.

Calculational Models and Procedures

In both cases the basic canister model is the standard configuration knockout canister described in B&W Document No. 77-1153937-03, Page 2-31. For conservatism, and to facilitate modeling in KENO standard geometry, the four satellite poison tubes and all lateral support plates are omitted and their space is occupied by fuel.

Additional conservatism is provided by assumptions of infinite extent of the canister array and enhancement of overhead reflection by concrete modeled above the array. A 17.3 inch square pitch was assumed.

For Case 1, the optimal fuel volume fraction was determined by NULIF calculations to be 0.620 with a K_∞ of 1.02890 and cell weighted cross sections for the KENO calculations were generated by NITAWL/XSDRNPM calculations.

For Case 2, a measured fuel volume fraction for randomly packed whole fuel pellets was used (B&W Commercial Plant License SNM-1168, Docket 70-1201, Section 3, Page 35). This volume fraction was 0.624 which by coincidence is close to that of Case 1. NULIF calculation for this volume fraction with saturated steam (pure H_2O) as moderator gave a K_∞ of 0.65706. Further NULIF calculations at this fuel volume fraction vs. increasing water density gave a monotomially increasing K_∞ up to 1.21412, at 100% water density. However, beyond the saturation point there would be liquid water not removed in the dewatering process and this water would be borated. This condition is covered in Case 1.

Results and Conclusions

For Case 1, the calculated maximum K_{eff}, including a 0.02 benchmark uncertainty and the 2σ KENO uncertainty, is 0.964. This is for an infinite X-Y array with no concrete side reflection. The effect of concrete reflection on the sides rather than an additional knockout canisters was shown to be negative with respect to reactivity.

For Case 2, the very low value of K_∞ compared to that for Case 3 assures that K_{eff} for an array of canister will be well below that for Case 1. This was verified by a KENO calculation for an infinite 17.3 inch pitch array yielding a value of K_{eff} of 0.632 including uncertainties. The effect of concrete reflection was found to be negative for this case also.

It is concluded that no realistically conceivable conditions that could occur during a TMI-2 storage pool drainage event would lead to a value of K_{eff} greater than the specified 0.99 acceptance criterion. This assumes that diluting or reflooding the canister contents with pure water is precluded by administrative control.